

# A Search for Outflows in the SEDIGISM survey

Aiyuan Yang & the SEDIGISM Team

# The SEDIGISM survey: a search for molecular outflows

A. Y. Yang<sup>1</sup>★, J. S. Urquhart<sup>2</sup>, F. Wyrowski<sup>1</sup>, M. A. Thompson<sup>3</sup>, C. König<sup>1</sup>, D. Colombo<sup>1</sup>, K. M. Menten<sup>1</sup>,  
A. Duarte-Cabral<sup>4</sup>, F. Schuller<sup>1,5</sup>, T. Csengeri<sup>6</sup>, D. Eden<sup>7</sup>, P. Barnes<sup>8,16</sup>, A. Traficante<sup>9</sup>, L. Bronfman<sup>10</sup>,  
A. Sanchez-Monge<sup>11</sup>, A. Ginsburg<sup>12</sup>, R. Cesaroni<sup>14</sup>, M.-Y. Lee<sup>13</sup>, H. Beuther<sup>15</sup>, S.-N. X. Medina<sup>1</sup>, P. Mazumdar<sup>1</sup>,  
T. Henning<sup>15</sup>

*Affiliations are listed in the end of the paper*

Received , ; accepted ,

# Outline

- Background
- Motivation
- Data analysis
- Main results
- Future Aspects
- Summary



Max-Planck-Institut  
für Radioastronomie

# Background: outflows

Snell+ 1980

- Star formation: collapse+accretion+outflows.
- Outflows
  - Injecting energy from few AU to several pc (Arce+2007).
  - the earliest observable signatures (e.g., Arce+2007).
  - First detection in 1976 (Zuckerman+1967), non-Gaussian molecular lines
  - High-velocity wings and spatially separated lobes at blue and red velocity shifted

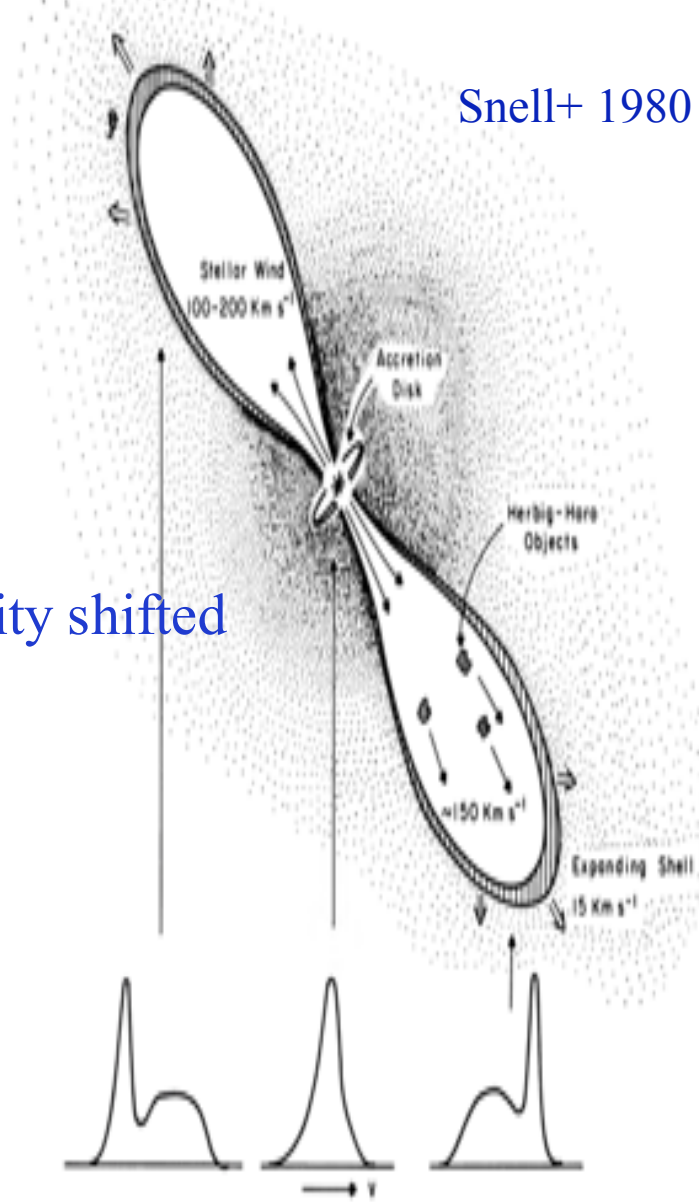
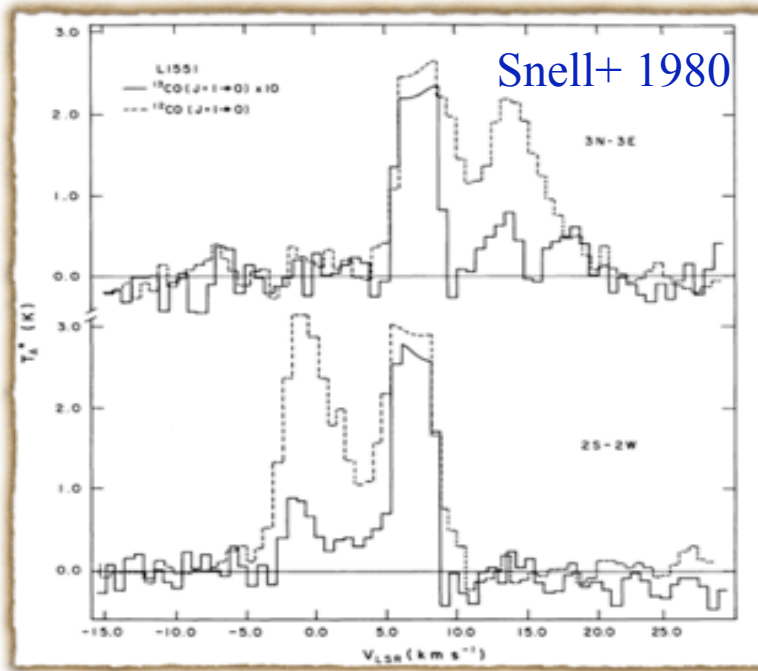
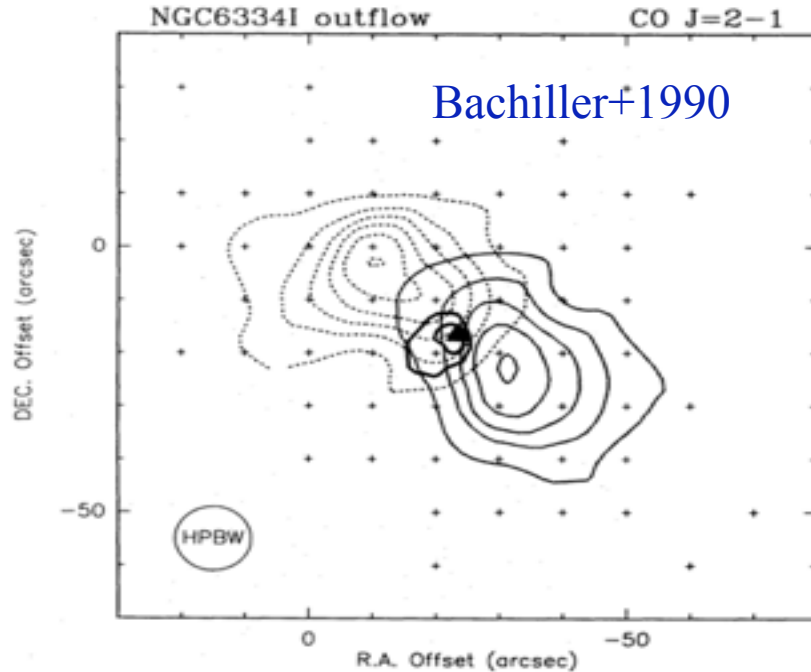


FIG. 5.—A schematic picture of the stellar wind driven shock model for L1551, indicating the CO line profiles which were obtained at different positions across the source. The Herbig-Haro objects are not necessarily located inside the shell; because of the velocities, they may have been ejected through the shell and into the surrounding medium.

# Background:outflows



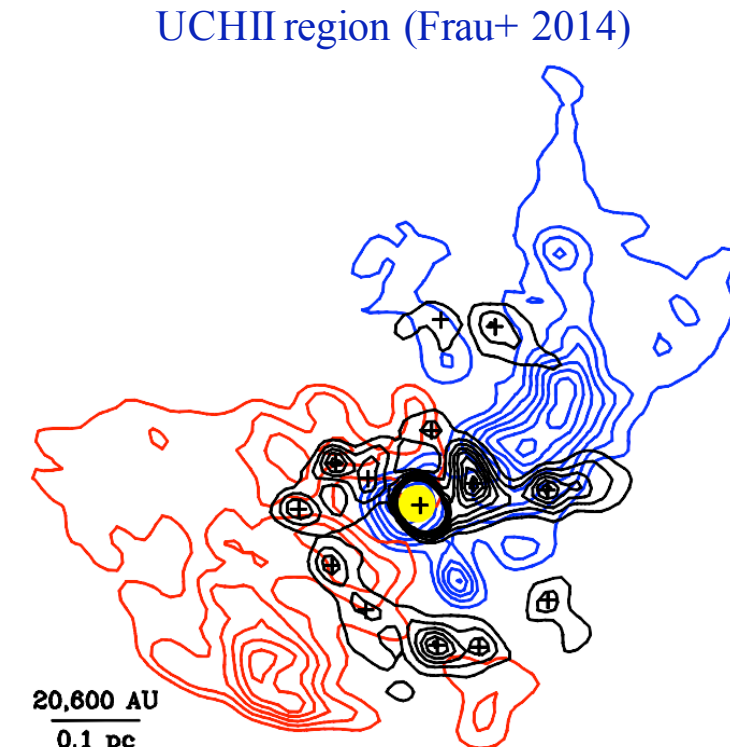
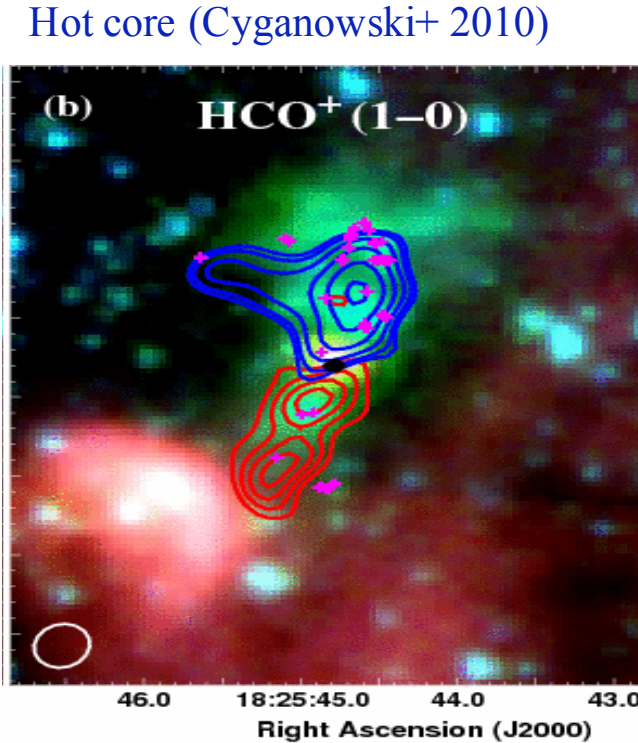
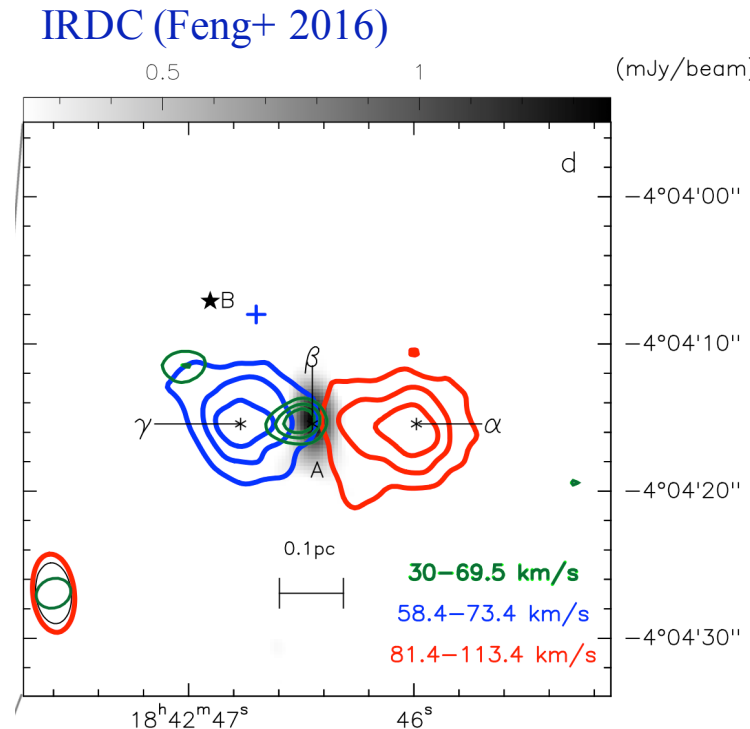
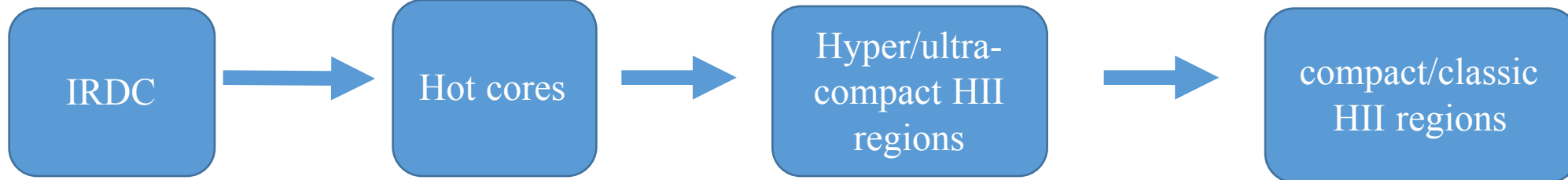
Max-Planck-Institut  
für Radioastronomie

- Therefore, outflow is a useful tool to understand star formation for all masses
  - High-mass star: high extinction + large distance + short timescale
    - How do massive star form?
    - Two competitive models:
    - Core Accretion? (e.g., McKee+2003) Or Competition accretion? (e.g., Bonnell +2001)
    - Massive collimated outflows VS less collimated outflows
  - Outflows
    - Theoretical models: highly ordered outflows of massive starless core candidate
    - Observations: outflows is observed from IRDC(Feng+2016) to UCHII(Codella+2004)

# Background: outflows

❖ Observations: Outflows have been observed in high-mass protostars

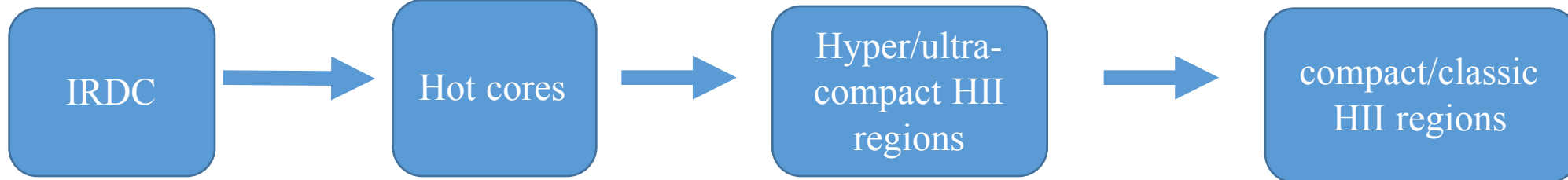
- Possible evolutionary sequences suggested by Zinnecker & Yorke 2007



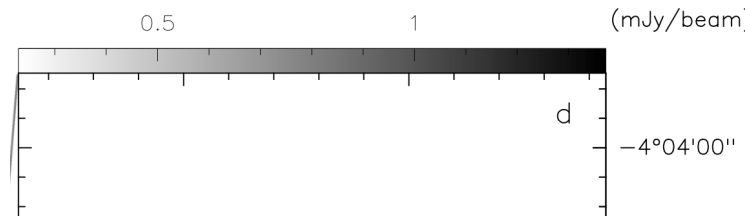
# Background: outflows

❖ Observations: Outflows have been observed in high-mass protostars

- Possible evolutionary sequences suggested by Zinnecker & Yorke 2007



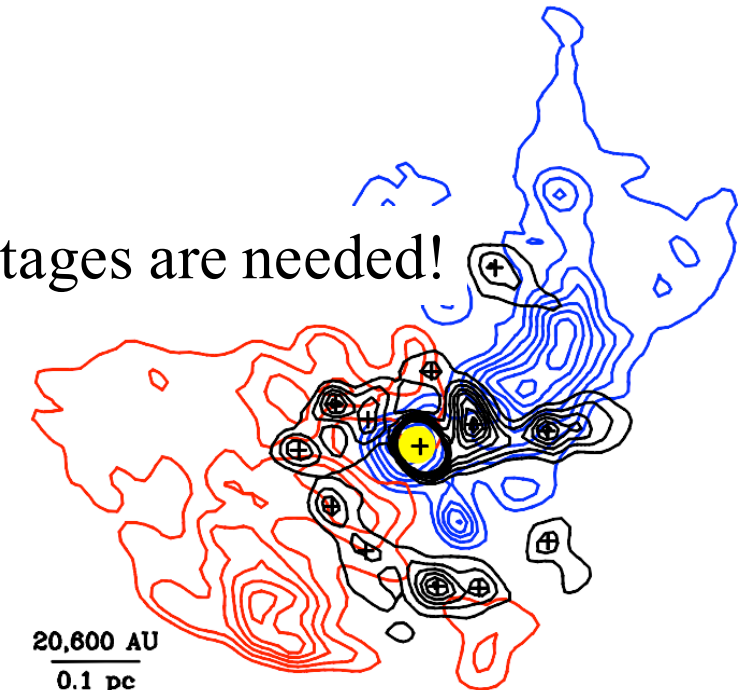
IRDC (Feng+ 2016)



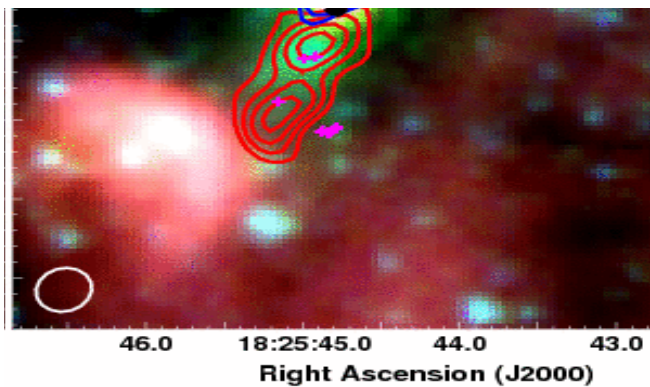
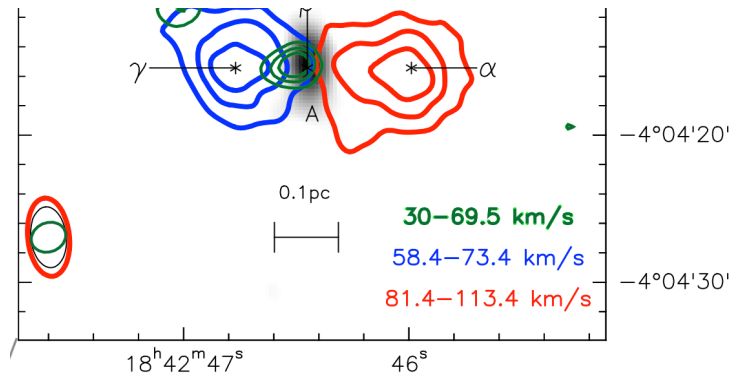
Hot core (Cyganowski+ 2010)



UCHII region (Frau+ 2014)



A significant samples of sources in different evolutionary stages are needed!

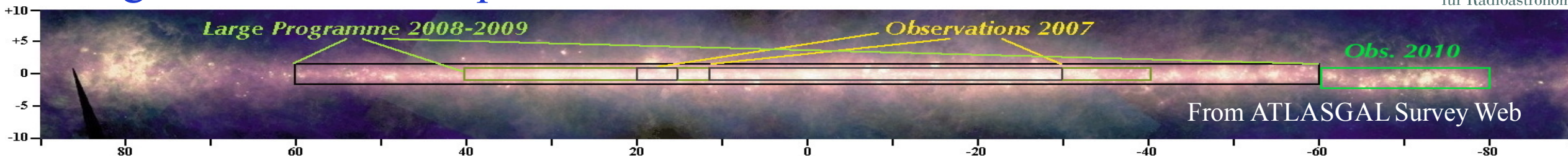


# Background: Outflows statistics

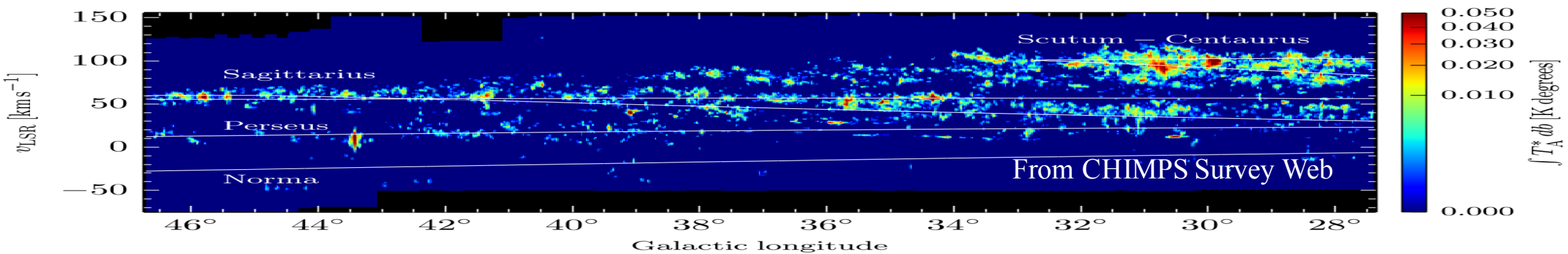


Max-Planck-Institut  
für Radioastronomie

- **ATLASGAL:** unbiased survey of massive star-forming clumps in a variety of stages in the Galactic plane.

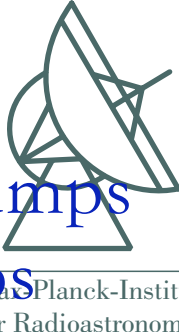


- **CHIMPS:** CO survey trace high density gas associated with star formation

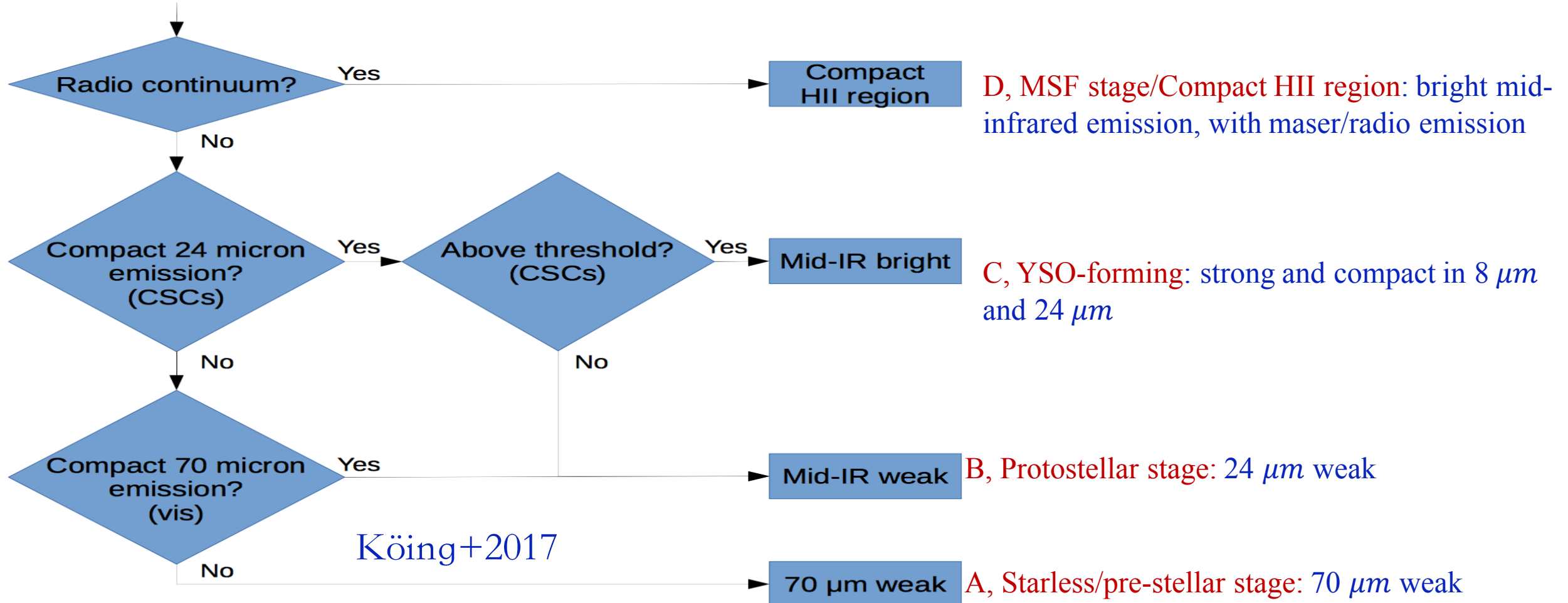


Names	Survey Area	Band	Sensitivity( $1\sigma$ )	Resolution	telescope	Ref.
CHIMPS	$28 < l < 46,  b  < 0.5$	$^{13}\text{CO} + \text{C}^{18}\text{O}$	0.6K	15''	JCMT	Rigby+ 2016
ATLSGAL	$180 < l < 60,  b  < 2$	$870\mu\text{m}$	50mJy	19''	APEX	Schuller+ 2009

# Background: Outflows statistics



- Köing+ 2017, Giannetti+ 2017: classify the evolutionary sequences for clumps
- Urquhart+ 2018: determine the physical properties for ATLASGAL clumps



# Background: Outflows properties



Planck-Institut  
für Radioastronomie

- 325 clumps  $\rightarrow$  225 with outflows  $\rightarrow$  153 can be used to determine outflow properties.
- Determination of outflow properties

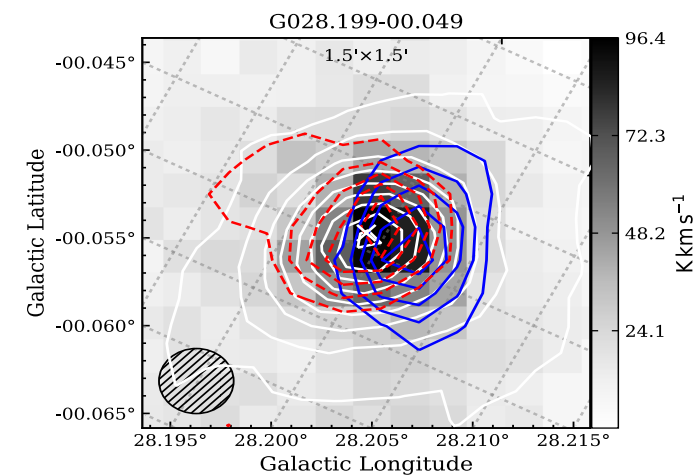
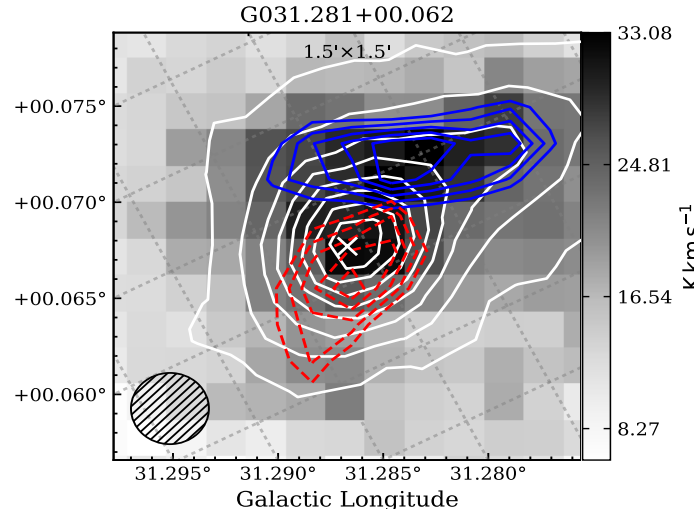
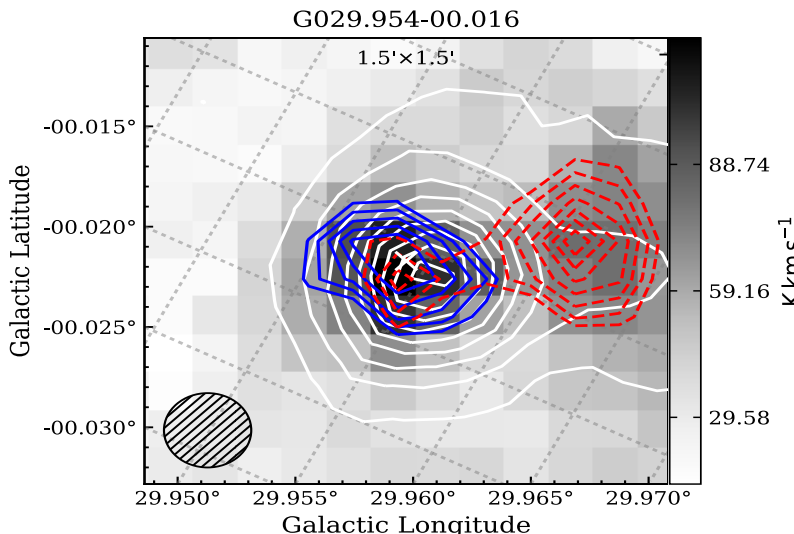
$$N(^{13}\text{CO}) = 5 \times 10^{12} T_{\text{ex}} \exp\left(\frac{T_{\text{trans}}}{T_{\text{ex}}}\right) \int T_{\text{mb}} dv (\text{cm}^{-2}), \quad (1)$$

$$M_{\text{out}} = M_r + M_b = (N_b \times A_b + N_r \times A_r) m_{H_2},$$

$$p = \sum_{A_b} \left[ \sum_{i=v_b} M_{b_i} v_i \right] \Delta v + \sum_{A_r} \left[ \sum_{i=v_r} M_{r_i} v_i \right] \Delta v \quad p = \sum_{A_b} \left[ \sum_{i=v_b} M_{b_i} v_i \right] \Delta v + \sum_{A_r} \left[ \sum_{i=v_r} M_{r_i} v_i \right] \Delta v \quad (4)$$

$$E = \frac{1}{2} \sum_{A_b} \left[ \sum_{i=v_b} M_{b_i} v_i^2 \right] \Delta v + \frac{1}{2} \sum_{A_r} \left[ \sum_{i=v_r} M_{r_i} v_i^2 \right] \Delta v \quad E = \frac{1}{2} \sum_{A_b} \left[ \sum_{i=v_b} M_{b_i} v_i^2 \right] \Delta v + \frac{1}{2} \sum_{A_r} \left[ \sum_{i=v_r} M_{r_i} v_i^2 \right] \Delta v. \quad (5)$$

$$t_d = \frac{l_{\text{max}}}{(V_{\text{maxb}} + V_{\text{maxr}})/2}.$$



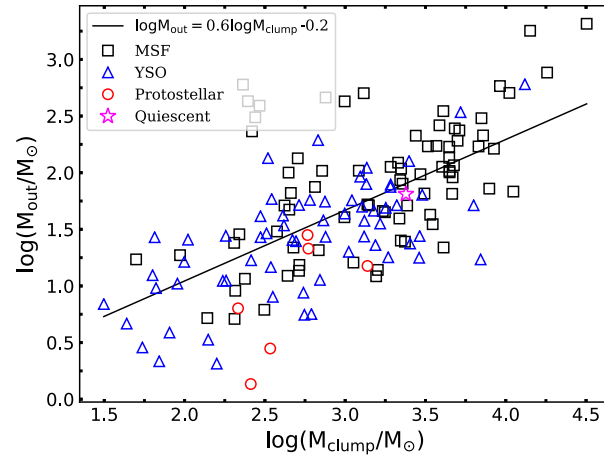
# Background: Outflows properties



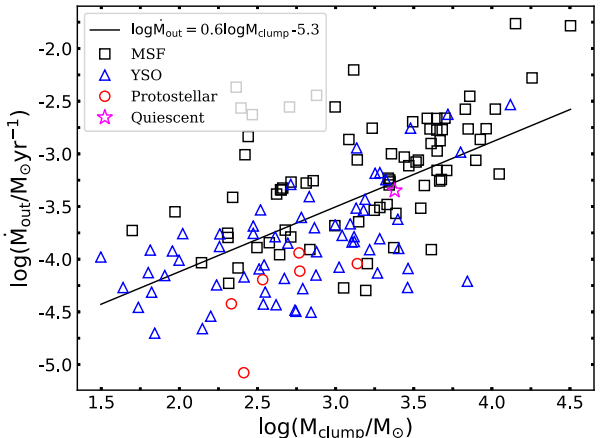
Max-Planck-Institut  
für Radioastronomie

- Outflows activity evolves with time—its properties at different stages
  - 3. Outflow properties as a function of the physical properties of clumps

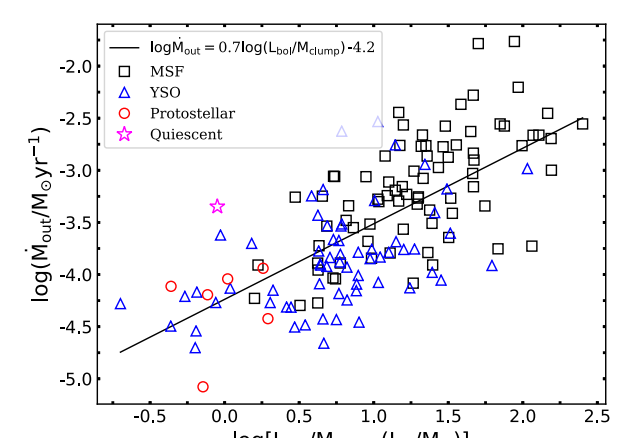
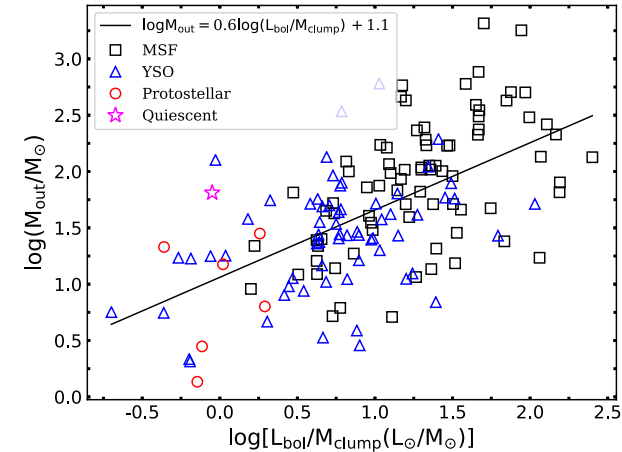
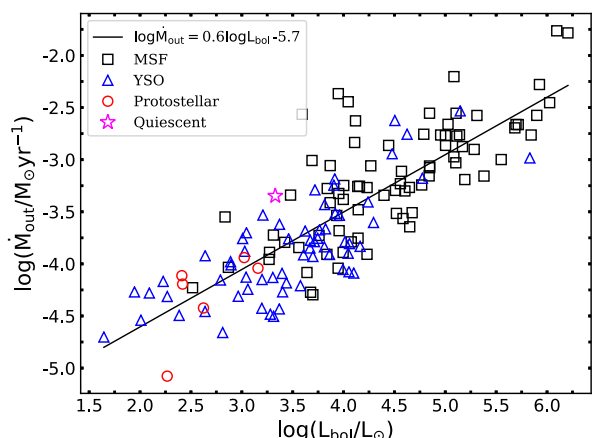
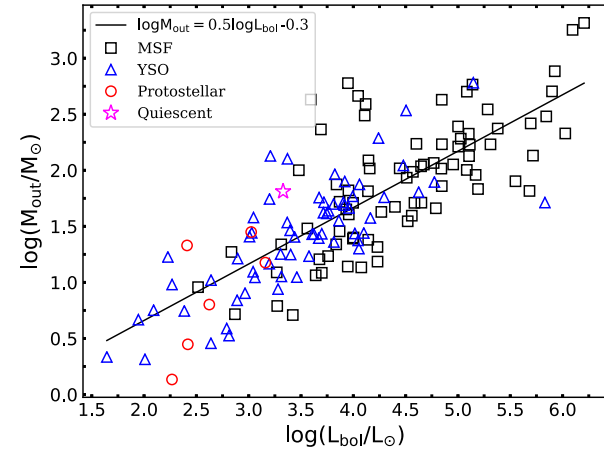
$M_{\text{out}} \propto \text{Clump}$



$\dot{M}_{\text{out}} \propto \text{Clump}$



Yang et al. 2018



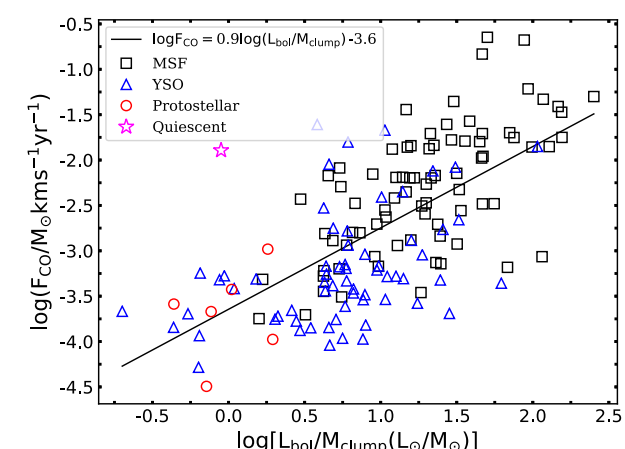
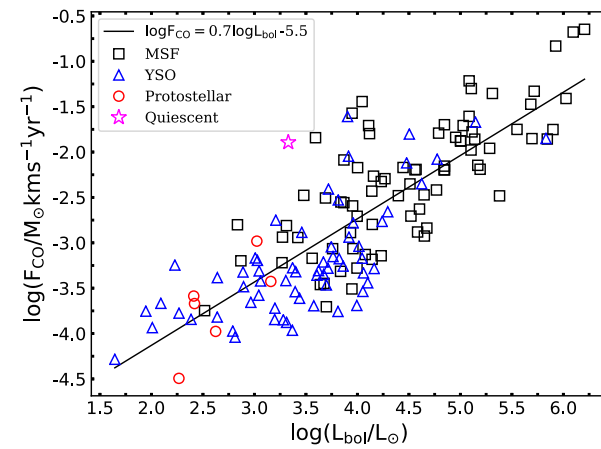
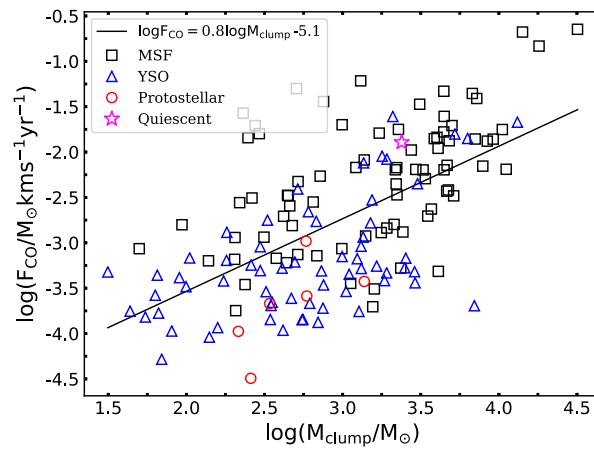
# Background: Outflows properties



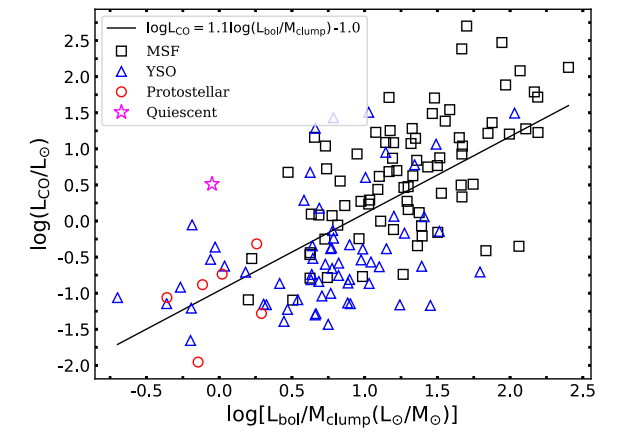
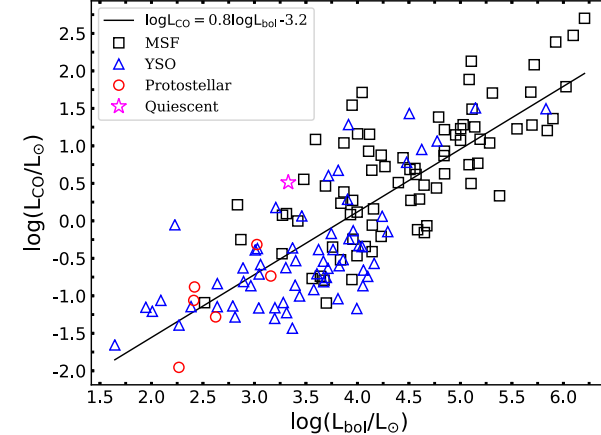
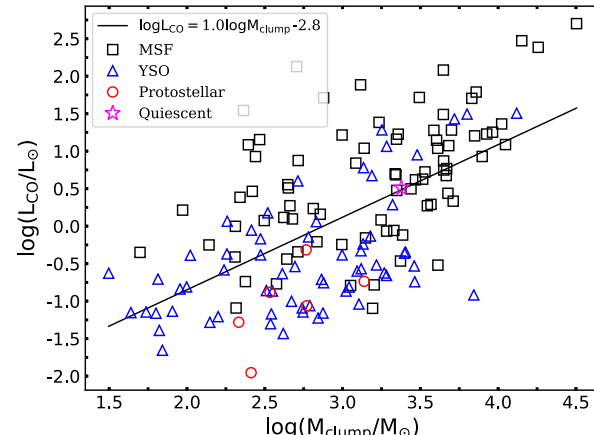
Max-Planck-Institut  
für Radioastronomie

- Outflows activity evolves with time—its properties at different stages
  - 3. Outflow properties as a function of the physical properties of clumps

$F_{CO} \propto$  Clump



$L_{CO} \propto$  Clump



Yang et al. 2018

# Background: Outflows properties

## ❖ Low-mass VS high-mass



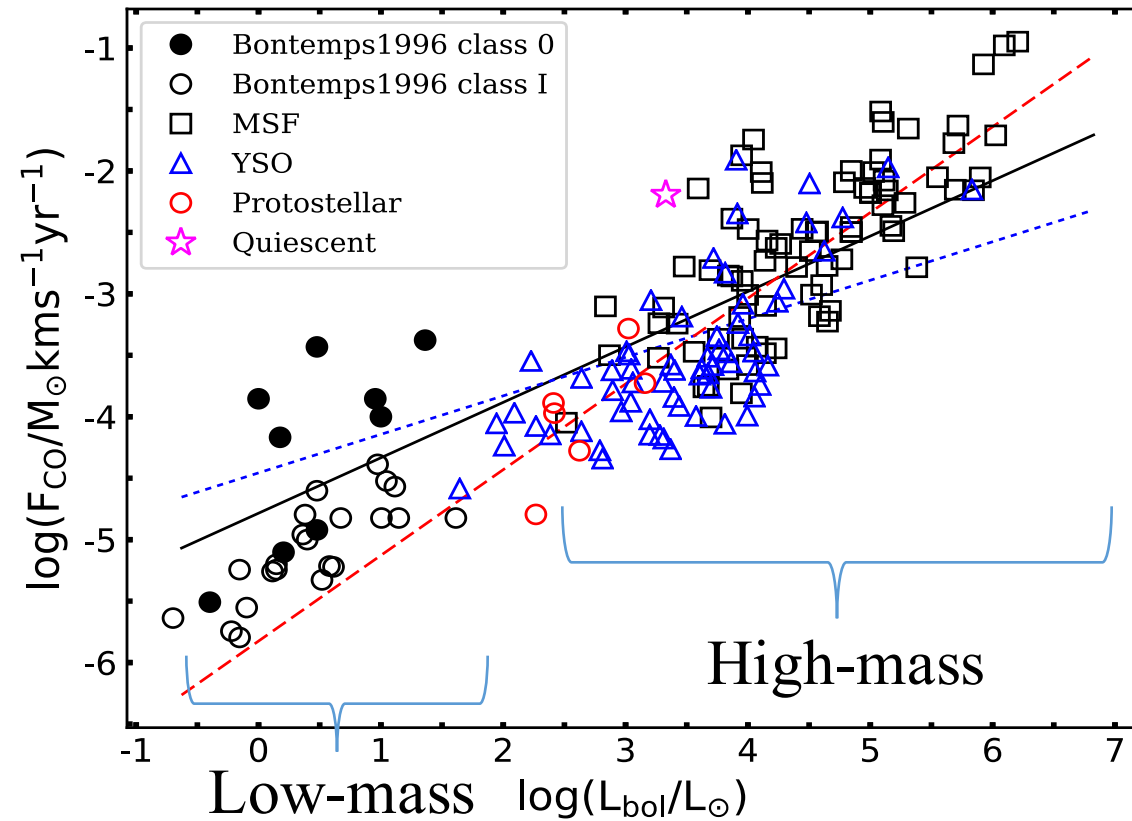
**Table 1**  
Typical Values for Low-mass and High-mass Outflows

Parameters	Low-mass Outflows <sup>a</sup>	High-mass Outflows <sup>b</sup>
$M_{\text{out}}$	$0.1 \sim 1 M_{\odot}$	$10 \sim 10^3 M_{\odot}$
$\dot{M}_{\text{out}}$	$10^{-7} \sim 10^{-6} M_{\odot} \text{ yr}^{-1}$	$10^{-5} \sim 10^{-3} M_{\odot} \text{ yr}^{-1}$
$F_{\text{out}}$	$10^{-6} \sim 10^{-5} M_{\odot} \text{ km s}^{-1} \text{ yr}^{-1}$	$10^{-4} \sim 10^{-2} M_{\odot} \text{ km s}^{-1} \text{ yr}^{-1}$
$L_{\text{out}}$	$0.1 \sim 1 L_{\odot}$	$0.1 \sim 100 L_{\odot}$
$\ell_{\text{out}}$	$0.1 \sim 1 \text{ pc}$	$0.5 \sim 2.5 \text{ pc}$
$t_{\text{d}}$	$(0.1 \sim 10) \times 10^5 \text{ years}$	$(0.1 \sim 10) \times 10^5 \text{ years}$

### Notes.

<sup>a</sup> E.g., Bontemps et al. (1996), Wu et al. (2004), Arce et al. (2007), Hatchell et al. (2007).

<sup>b</sup> E.g., Richer et al. (2000), Beuther et al. (2002), Wu et al. (2004), Zhang et al. (2005), Kim & Kurtz (2006), Arce et al. (2007), de Villiers et al. (2014), de Villiers et al. (2015), Maud et al. (2015).



A statistically significant samples of clumps in the early evolutionary stages are needed!

# Two Surveys

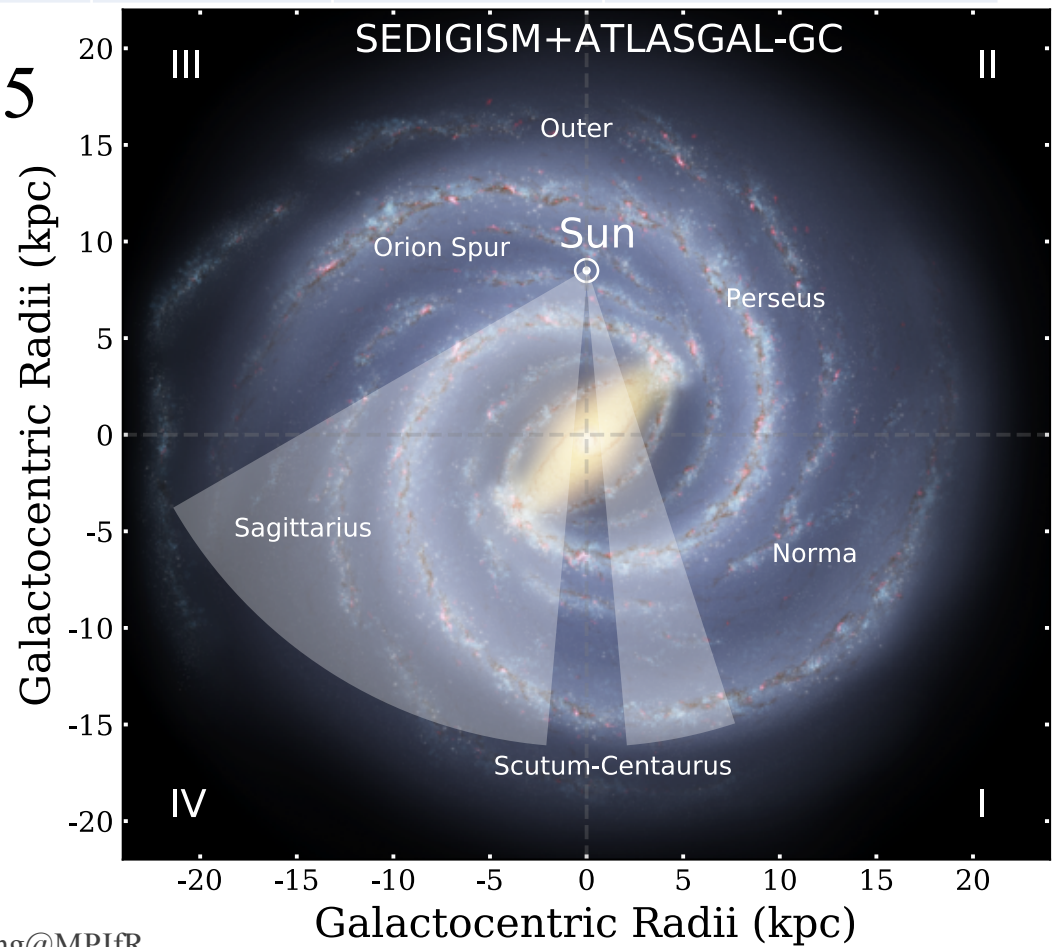


Max-Planck-Institut  
für Radioastronomie

Names	Survey Area	Band	Sensitivity( $1\sigma$ )	Resolution	telescope	Ref.
SEDIGISM	$-60 < l < 18^\circ,  b  < 0.5^\circ$	$^{13}\text{CO} + \text{C}^{18}\text{O}$	0.8K	28''	APEX	Schuller+ 2017
ATLASGAL	$ \ell  < 60^\circ,  b  < 1.5^\circ$	$870\mu\text{m}$	50mJy	19''	APEX	Schuller+ 2009

Overlap sky region:  $-60 < l < 18; |b| < 0.5$

Excluding GC: 68 square degree!



# Two Surveys

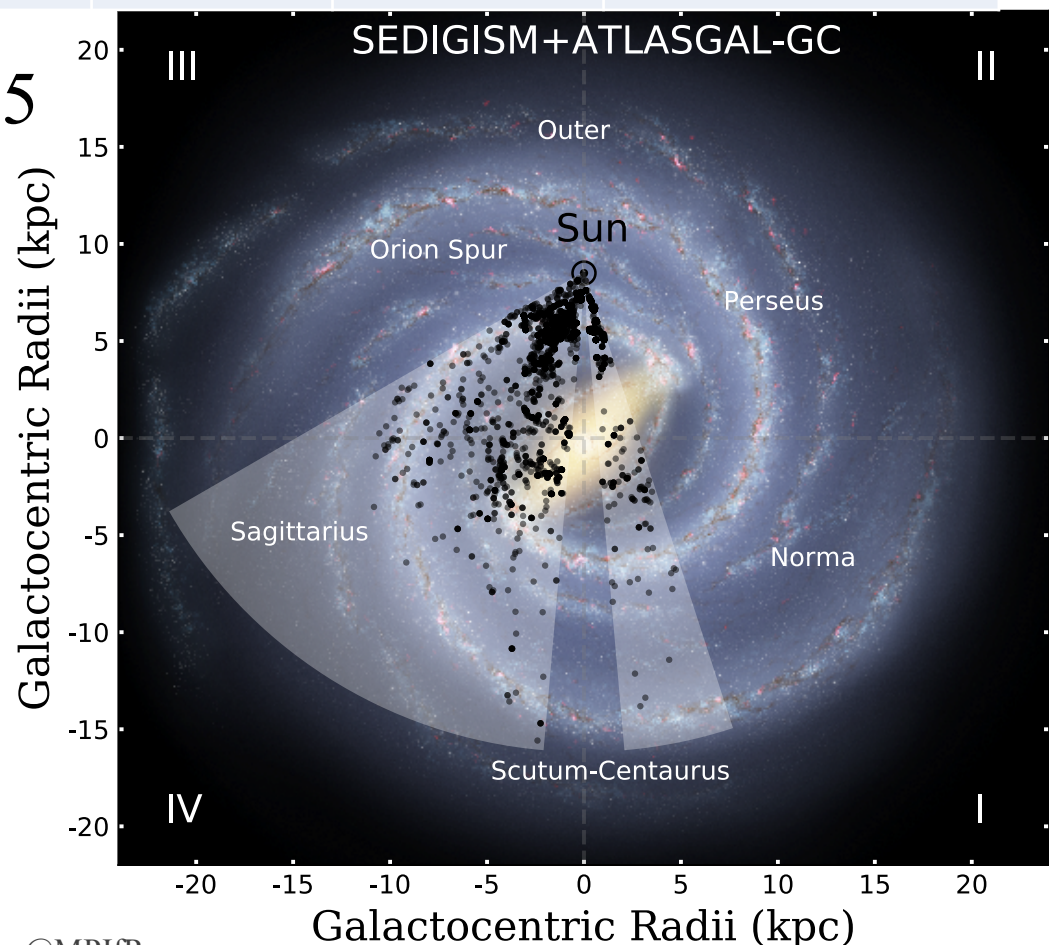
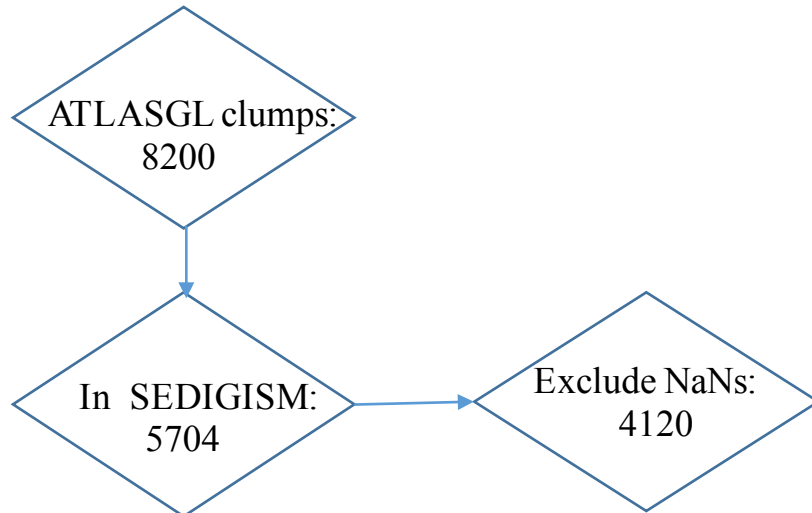


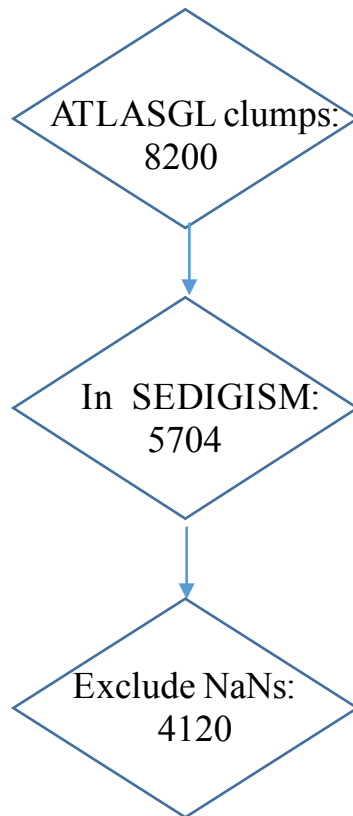
Max-Planck-Institut  
für Radioastronomie

Names	Survey Area	Band	Sensitivity( $1\sigma$ )	Resolution	telescope	Ref.
SEDIGISM	$-60 < l < 18^\circ,  b  < 0.5^\circ$	$^{13}\text{CO} + \text{C}^{18}\text{O}$	0.8K	28''	APEX	Schuller+ 2017
ATLASGAL	$ \ell  < 60^\circ,  b  < 1.5^\circ$	$870\mu\text{m}$	50mJy	19''	APEX	Schuller+ 2009

Overlap sky region:  $-60 < l < 18; |b| < 0.5$

Excluding GC: 68 square degree!

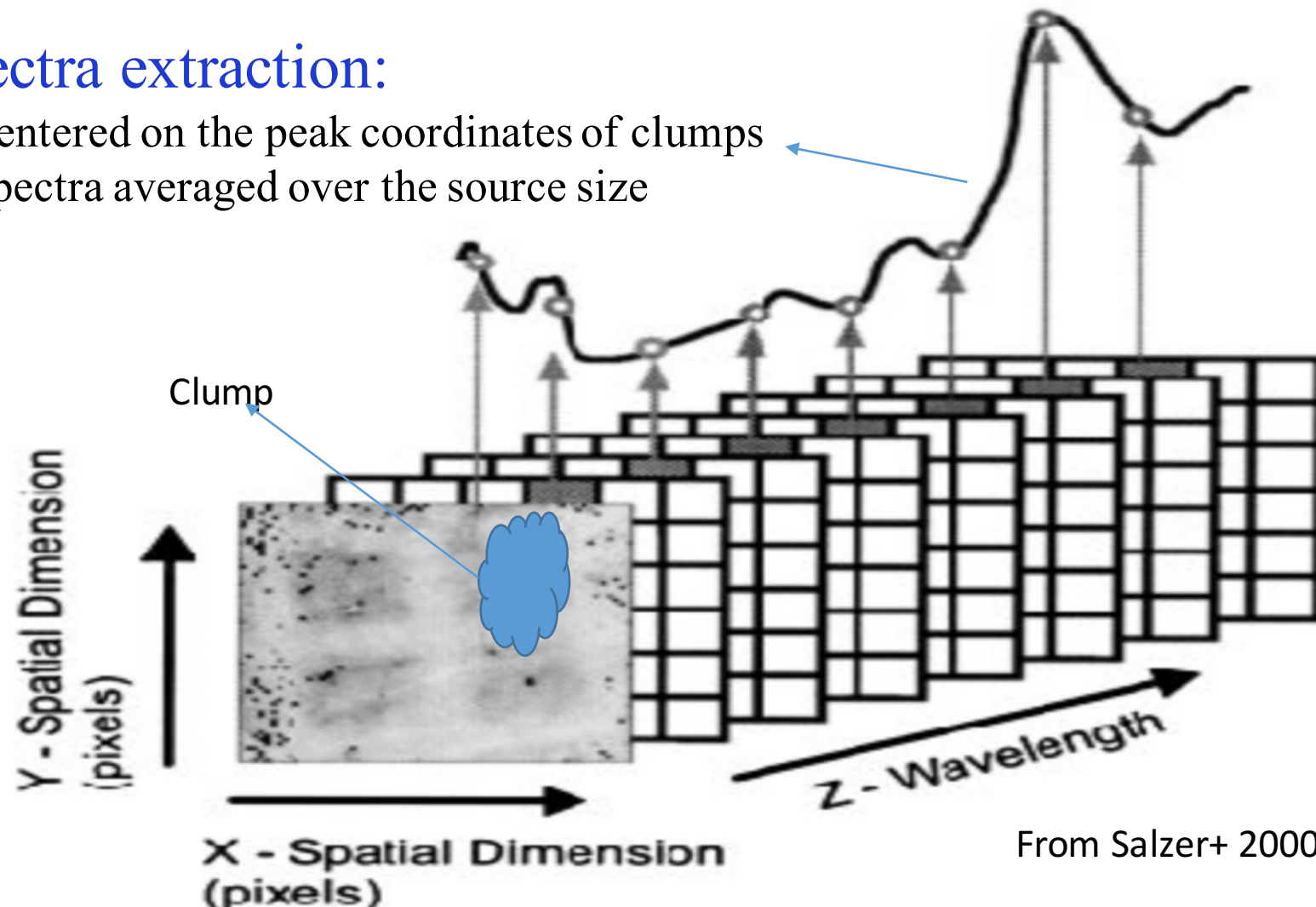


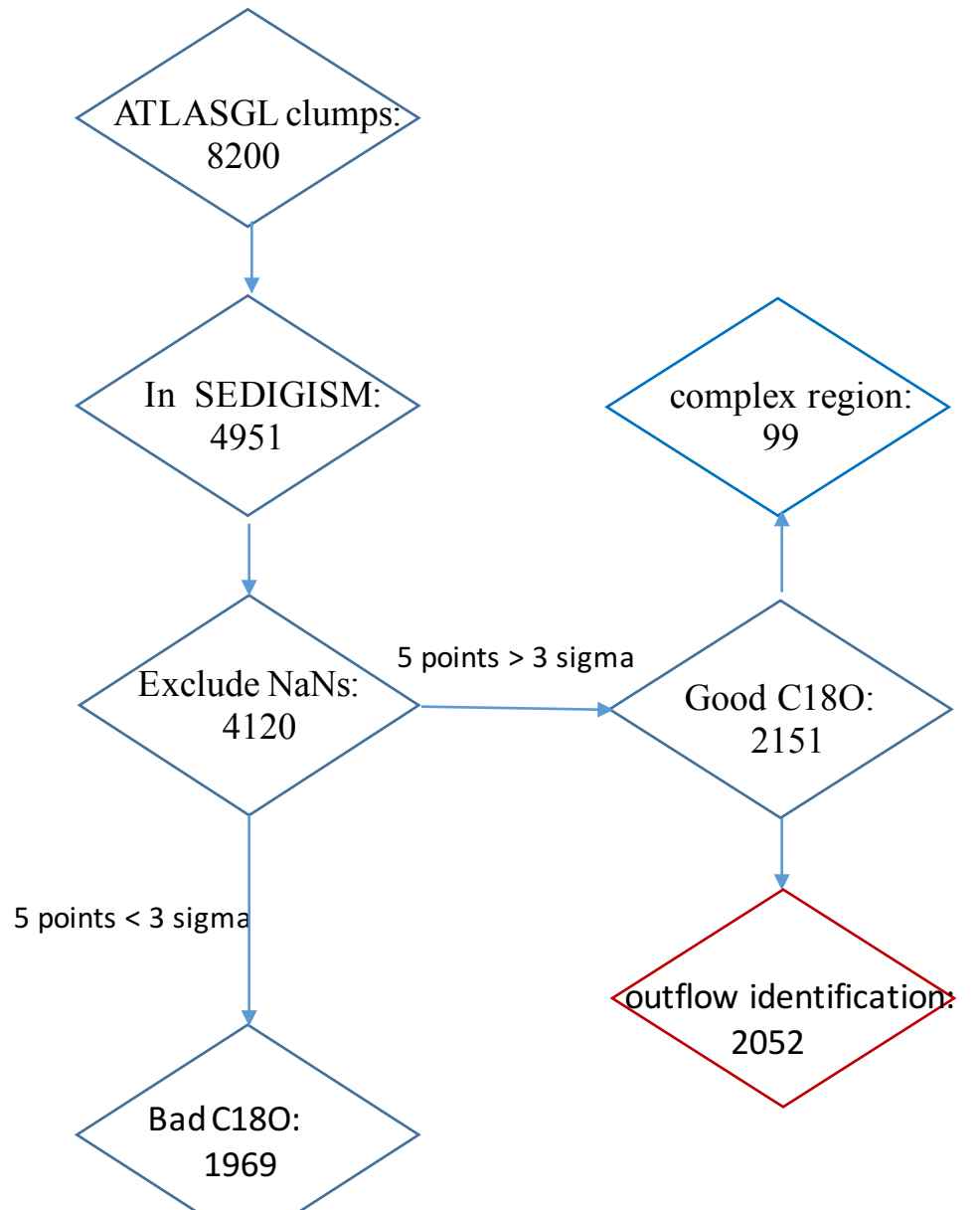


Surveys	Freq./Beam	Rms( $1\sigma$ )	Sky coverage
ATLASGAL	345GHz@19"	$\sim 50\text{mJy}$	$-60 < l < 60;  b  < 2$
SEDIGISM	219GHz@28"	$\sim 0.8\text{K}@0.25\text{km/s}$	$-60 < l < 18;  b  < 0.5$

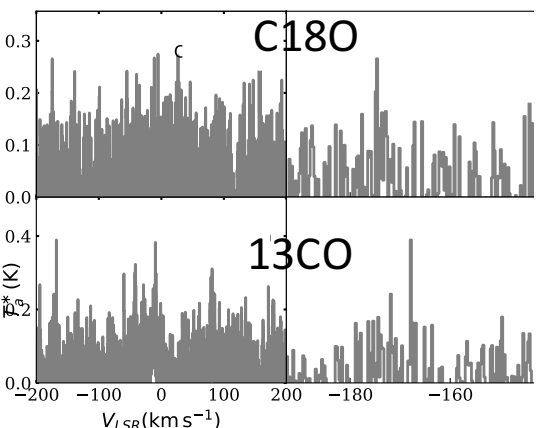
## Spectra extraction:

- Centered on the peak coordinates of clumps
- Spectra averaged over the source size

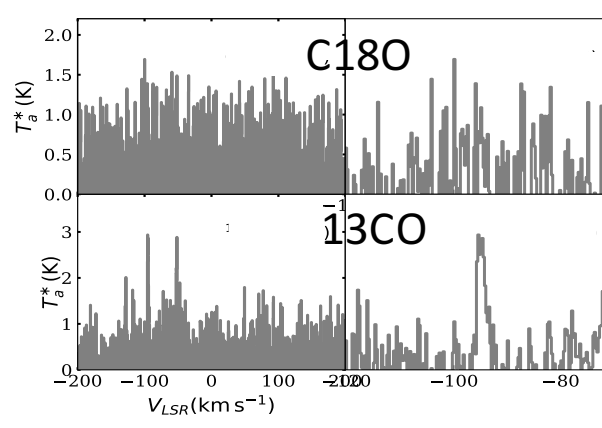




1, No C18O & No 13CO : 147

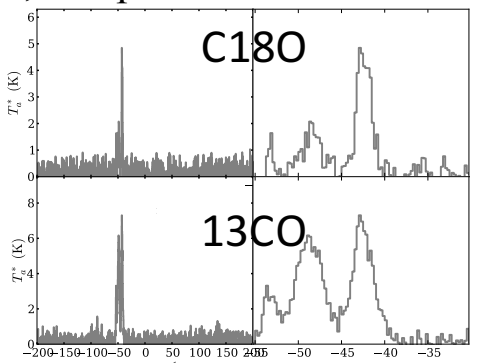


2, No/weak C18O & Weak 13CO : 1969

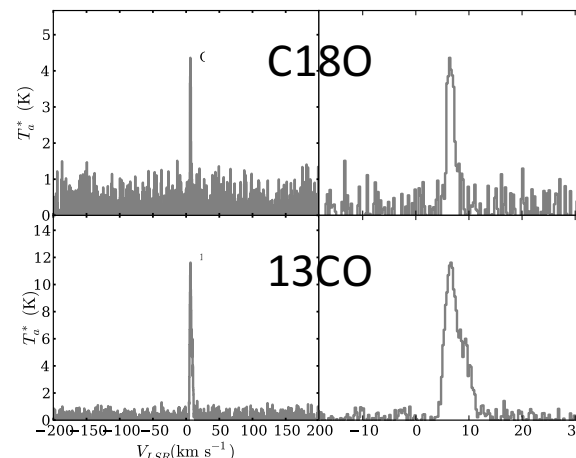
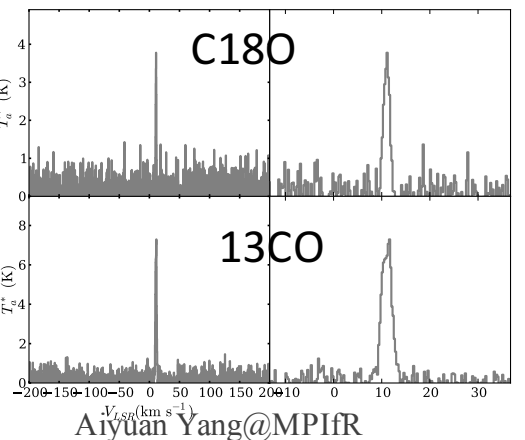


Max-Planck-Institut  
für Radioastronomie

3, complex C18O & / 13CO : 99

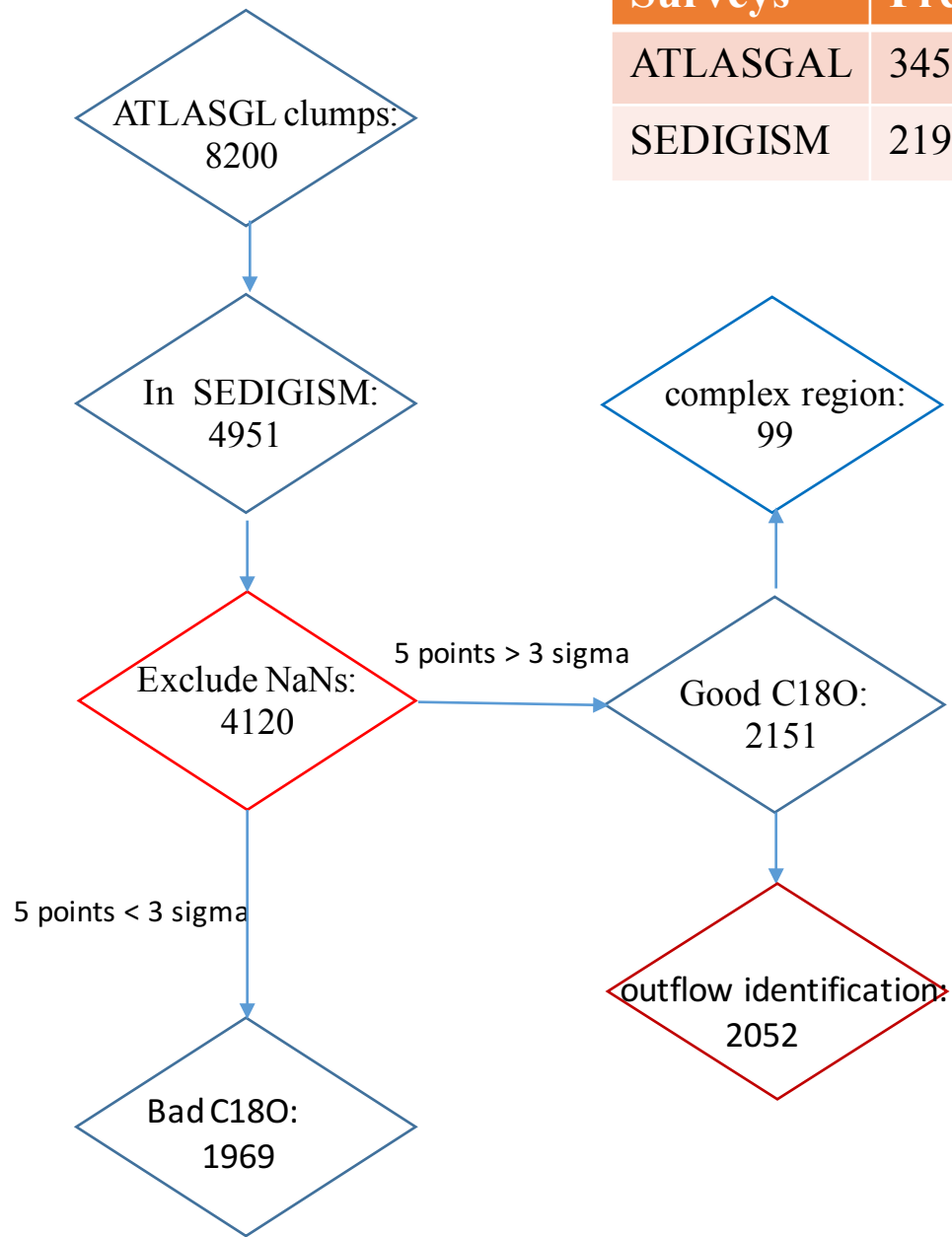


4, used C18O & 13CO : 2057

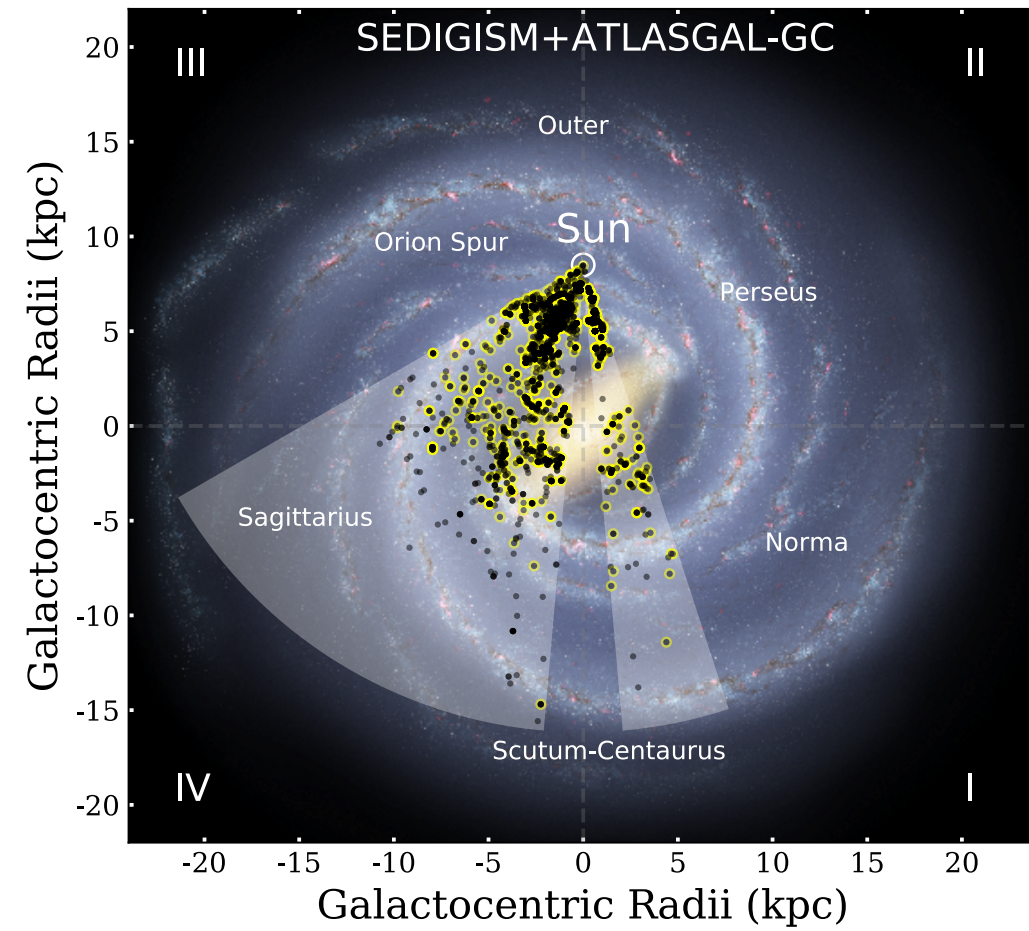




itut  
mie



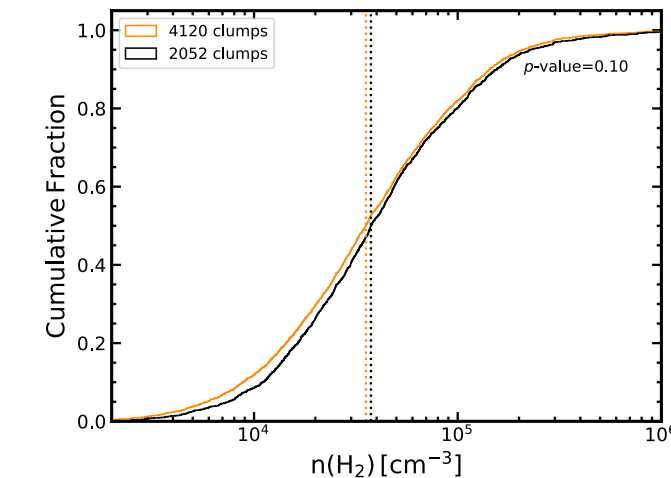
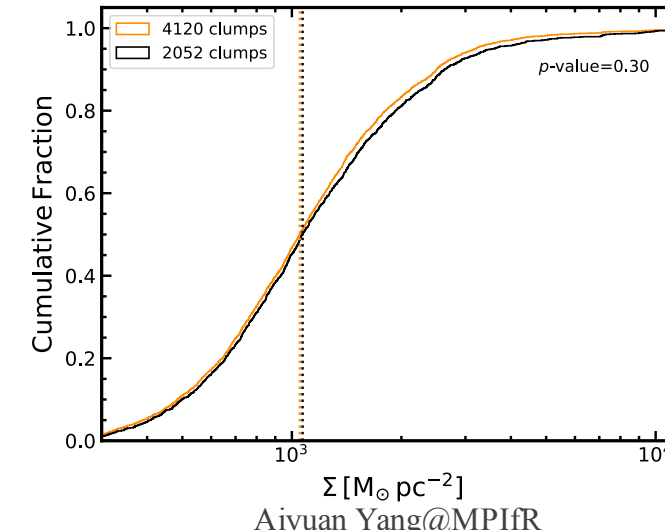
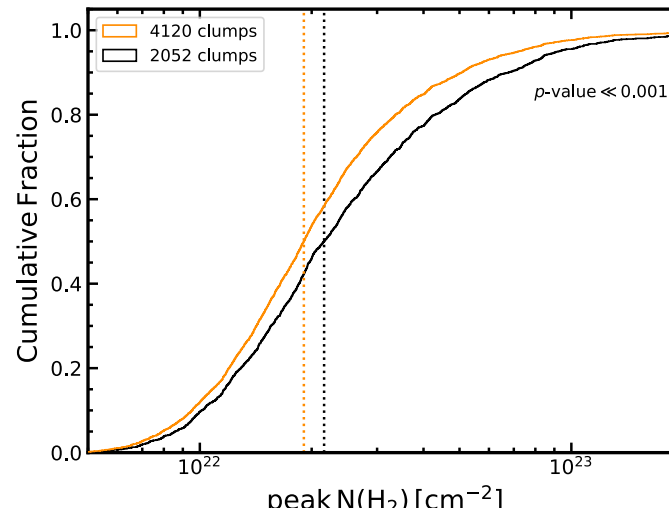
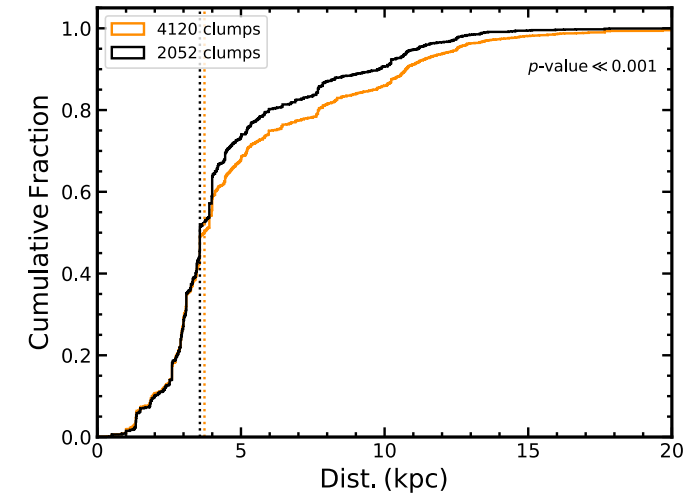
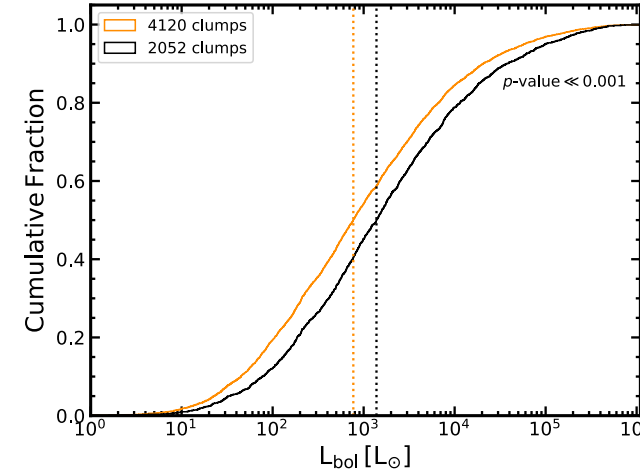
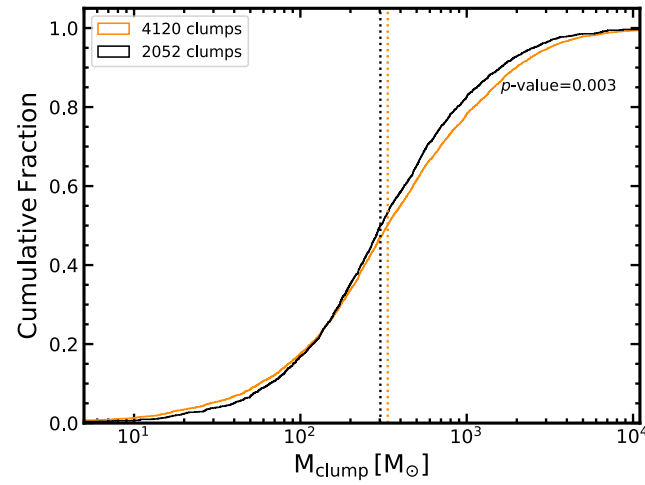
Surveys	Freq./Beam	Rms( $1\sigma$ )	Sky coverage
ATLASGAL	345GHz@19"	$\sim 50\text{mJy}$	$-60 \leq l \leq 60;  b  \leq 2$
SEDIGISM	219GHz@28"	$\sim 0.8\text{K}@0.25\text{km/s}$	$-60 \leq l \leq 18;  b  \leq 0.5$



# The selected sample VS the total sample



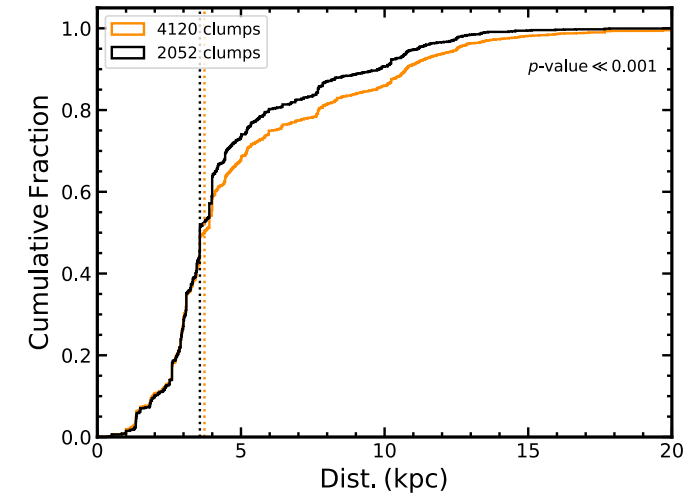
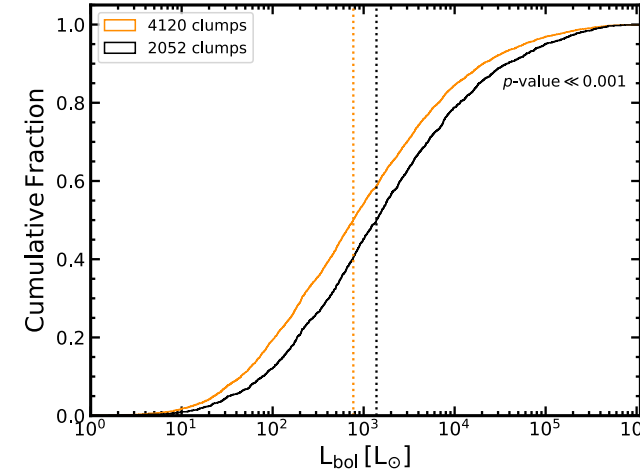
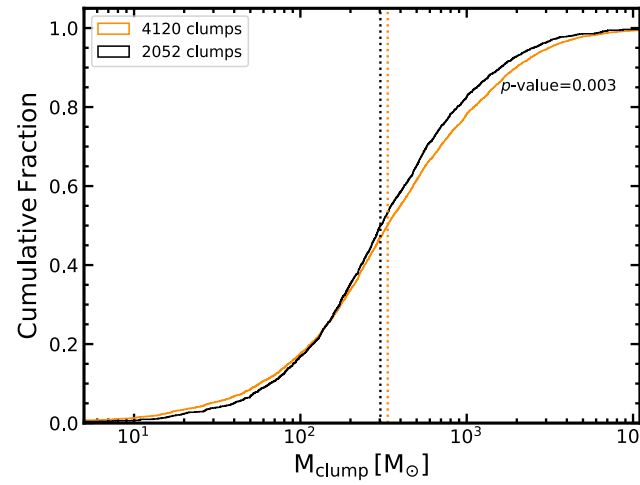
Planck-Institut  
für Radioastronomie



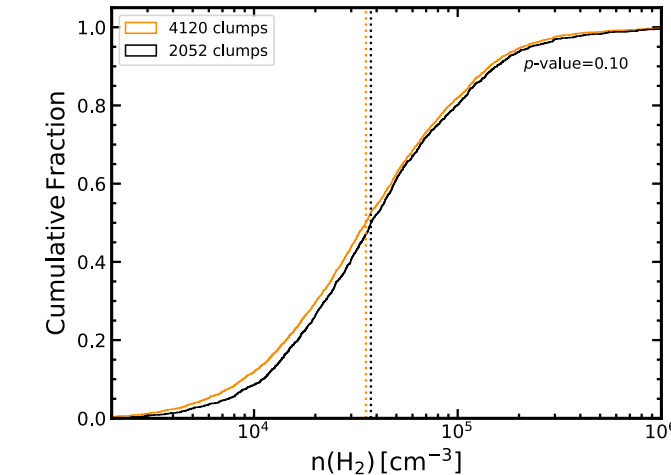
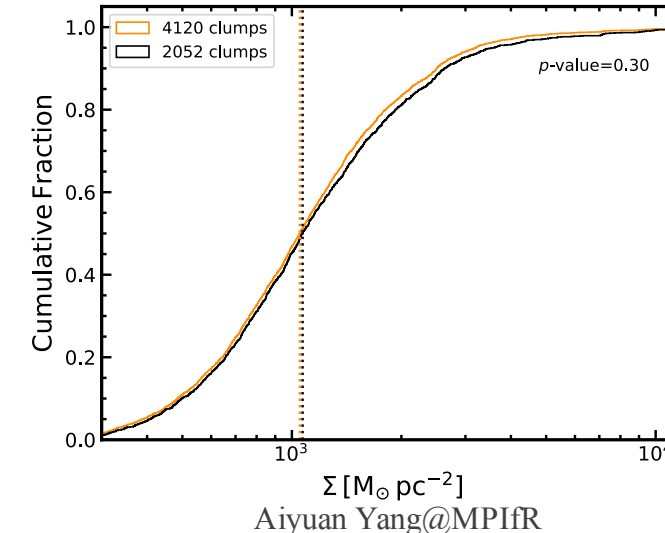
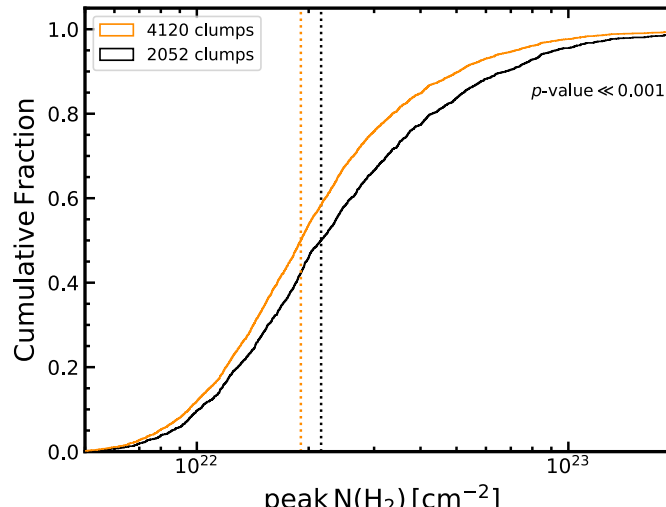
# The selected sample VS the total sample



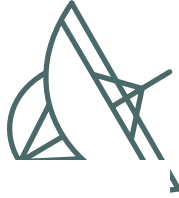
Planck-Institut  
für Radioastronomie



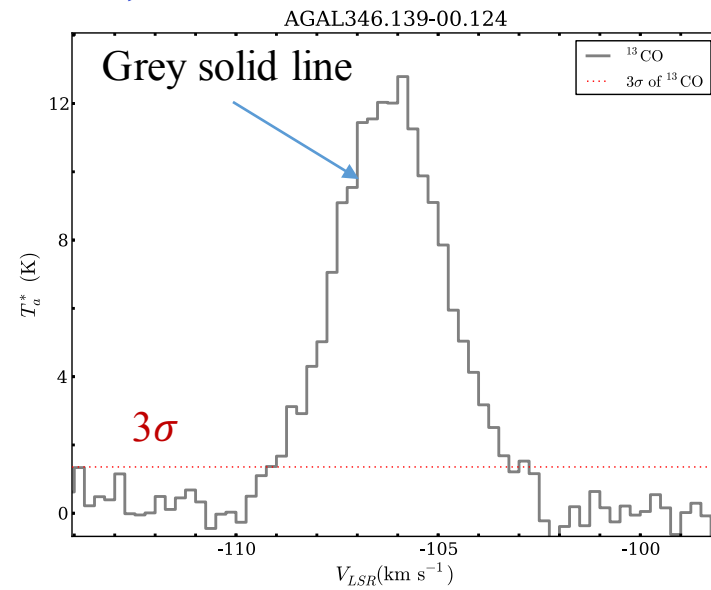
The selected clumps are closer and brighter than the total clumps.



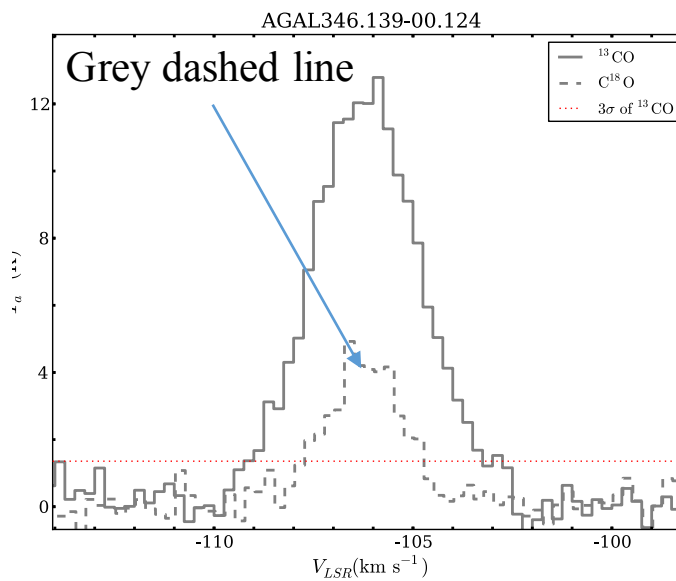
- Outflows identification:  $^{13}\text{CO}$ : high-velocity wings;  $\text{C}^{18}\text{O}$ : core emission



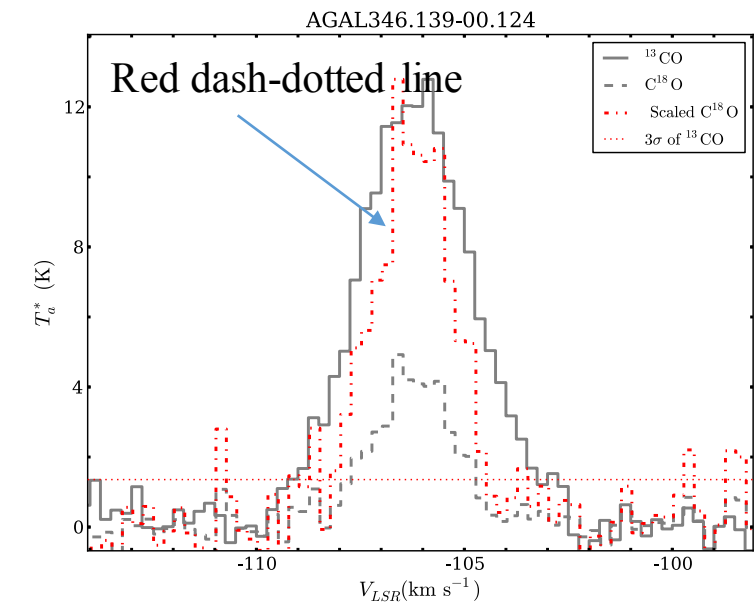
1,  $^{13}\text{CO}$  emission



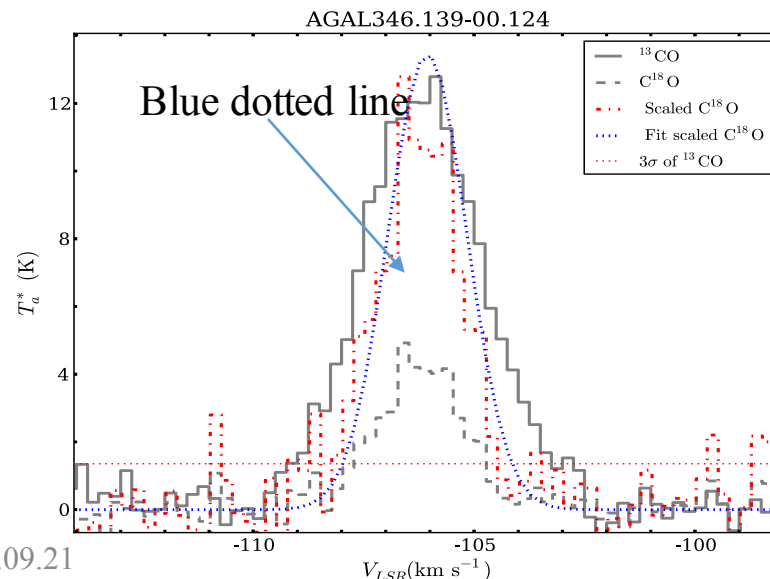
2,  $\text{C}^{18}\text{O}$  emission



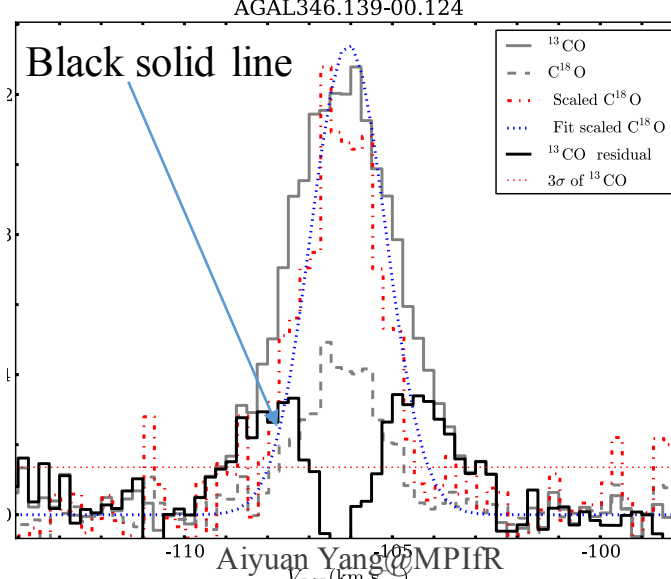
3, scaled  $\text{C}^{18}\text{O}$  emission



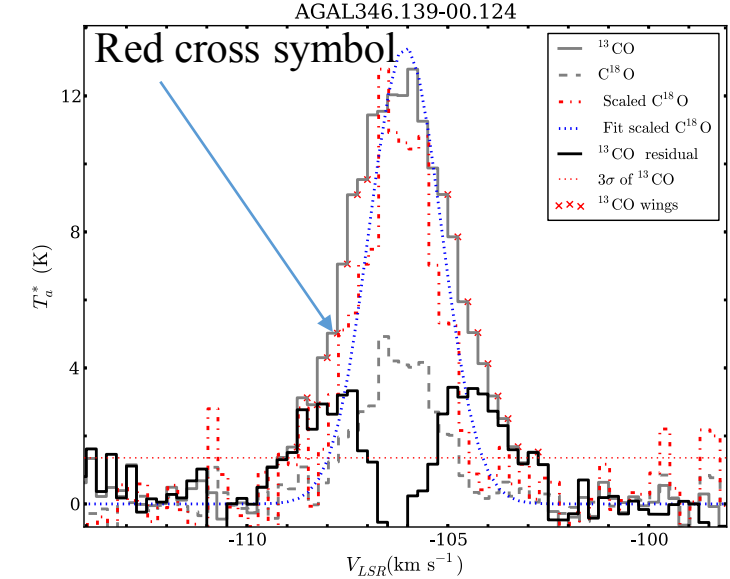
4, Gaussian fitting to scaled  $\text{C}^{18}\text{O}$



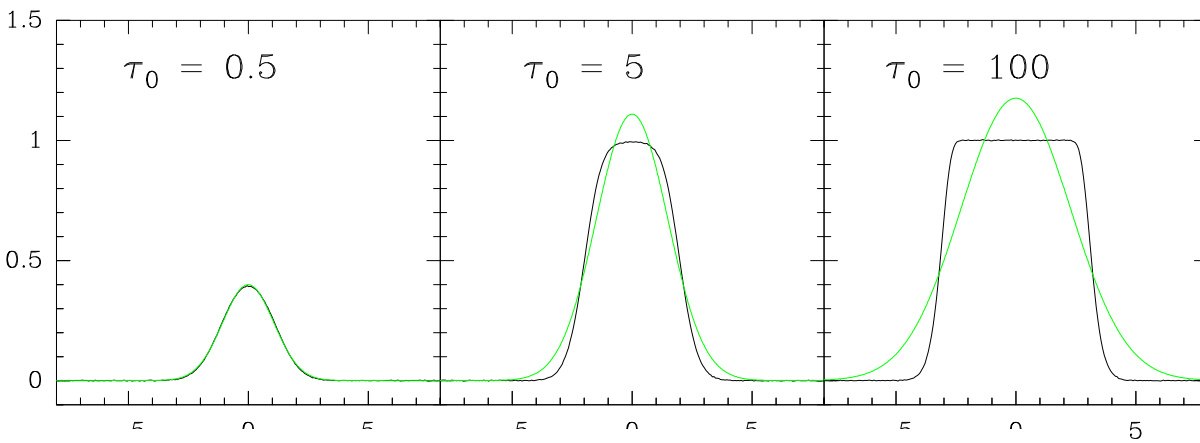
5,  $(^{13}\text{CO}) - (\text{fitted-scaled } \text{C}^{18}\text{O})$



6, Outflow high-velocity wings



# • Outflows identification: opacity broadening

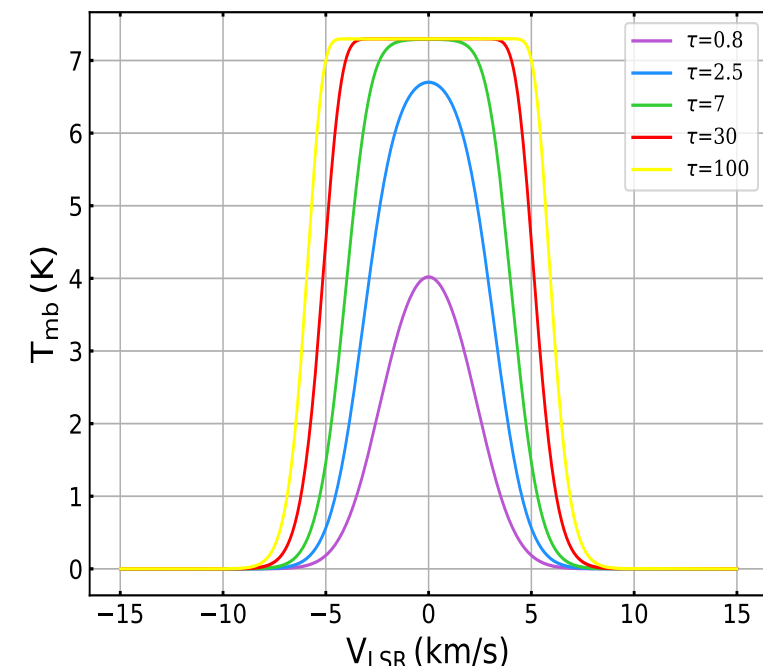
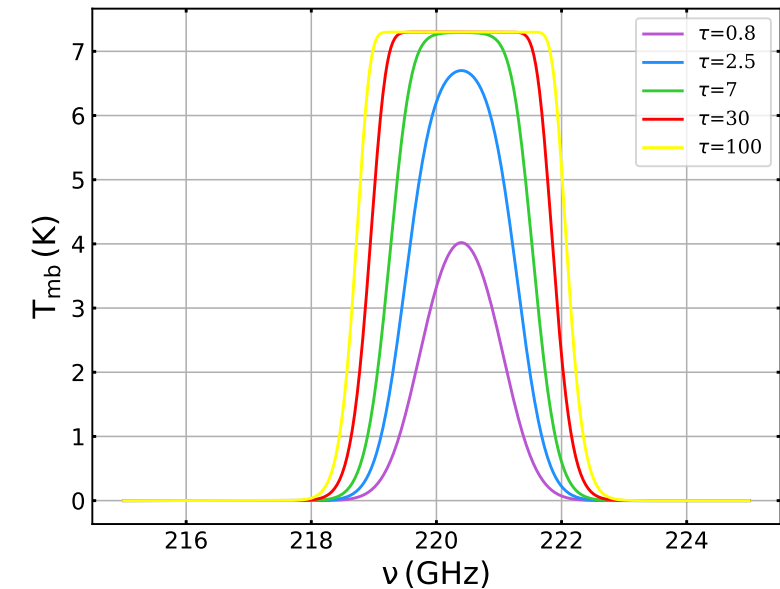


$$T_{\text{mb},\nu} = (J_\nu(T_{\text{ex}}) - J_\nu(T_{\text{bg}})) \cdot (1 - \exp(-\tau_\nu)),$$

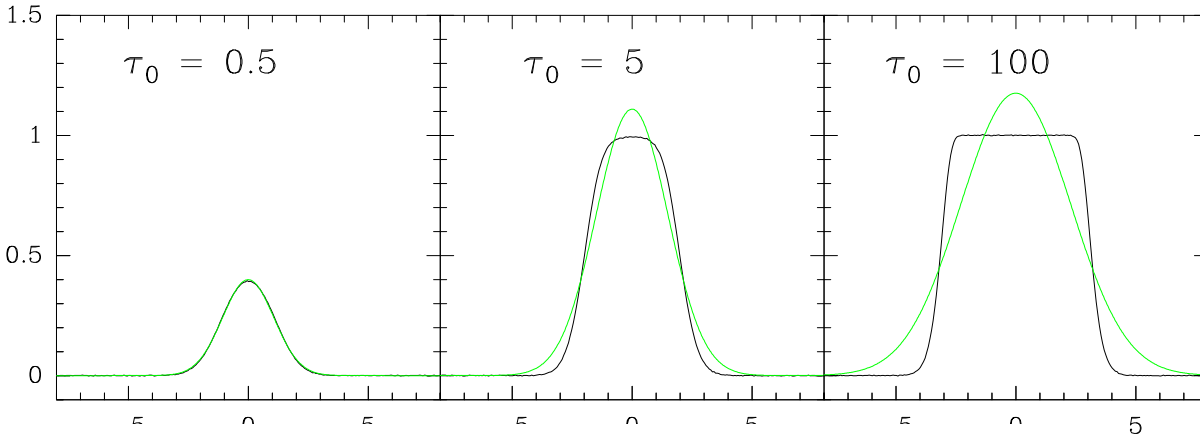
The line opacity follows a Gaussian distribution as:

$$\tau_\nu = \tau_0 \cdot \exp(-(v - v_0)^2 / 2\sigma^2)$$

$$\frac{v - v_0}{v_0} = \frac{v_{\text{lsr}} - v_{\text{lsr},0}}{c}$$



## • Outflows identification: opacity broadening



$$T_{\text{mb},\nu} = (J_\nu(T_{\text{ex}}) - J_\nu(T_{\text{bg}})) \cdot (1 - \exp(-\tau_\nu)),$$

The line opacity follows a Gaussian distribution as:

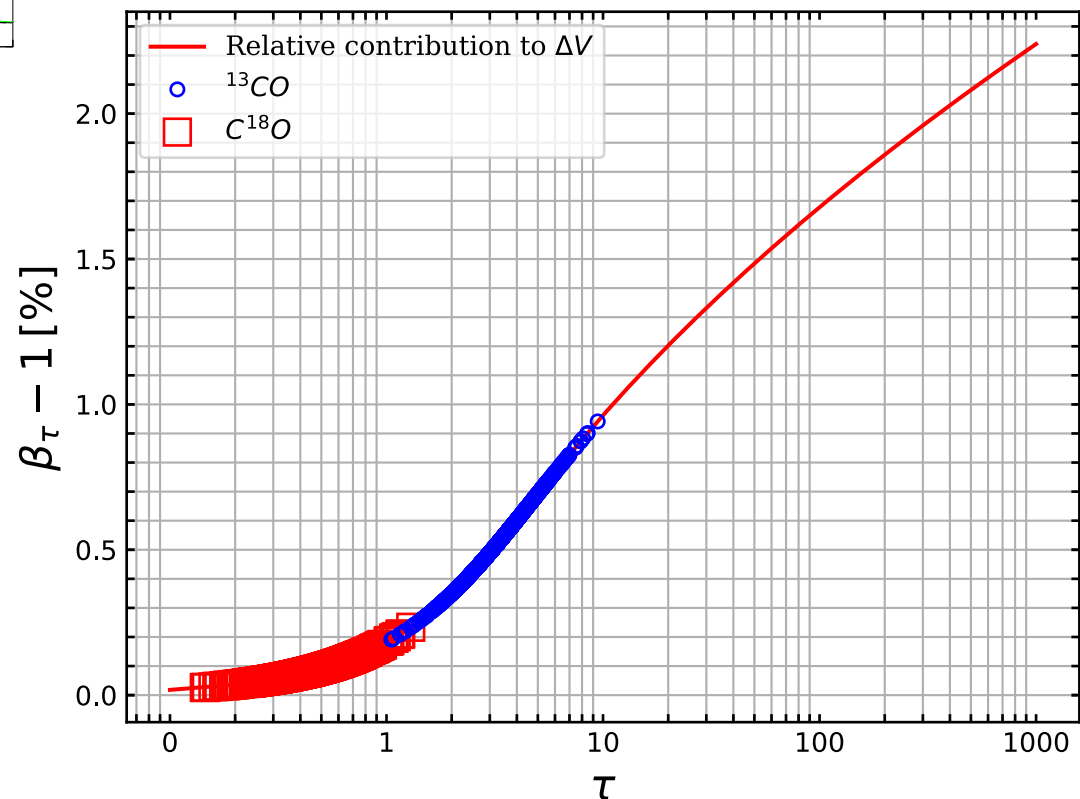
$$\tau_\nu = \tau_0 \cdot \exp(-(v - v_0)^2 / 2\sigma^2)$$

$$\frac{v - v_0}{v_0} = \frac{v_{\text{lsr}} - v_{\text{lsr,0}}}{c}$$

- FWHM(observed)/FWHM(intrinsic)

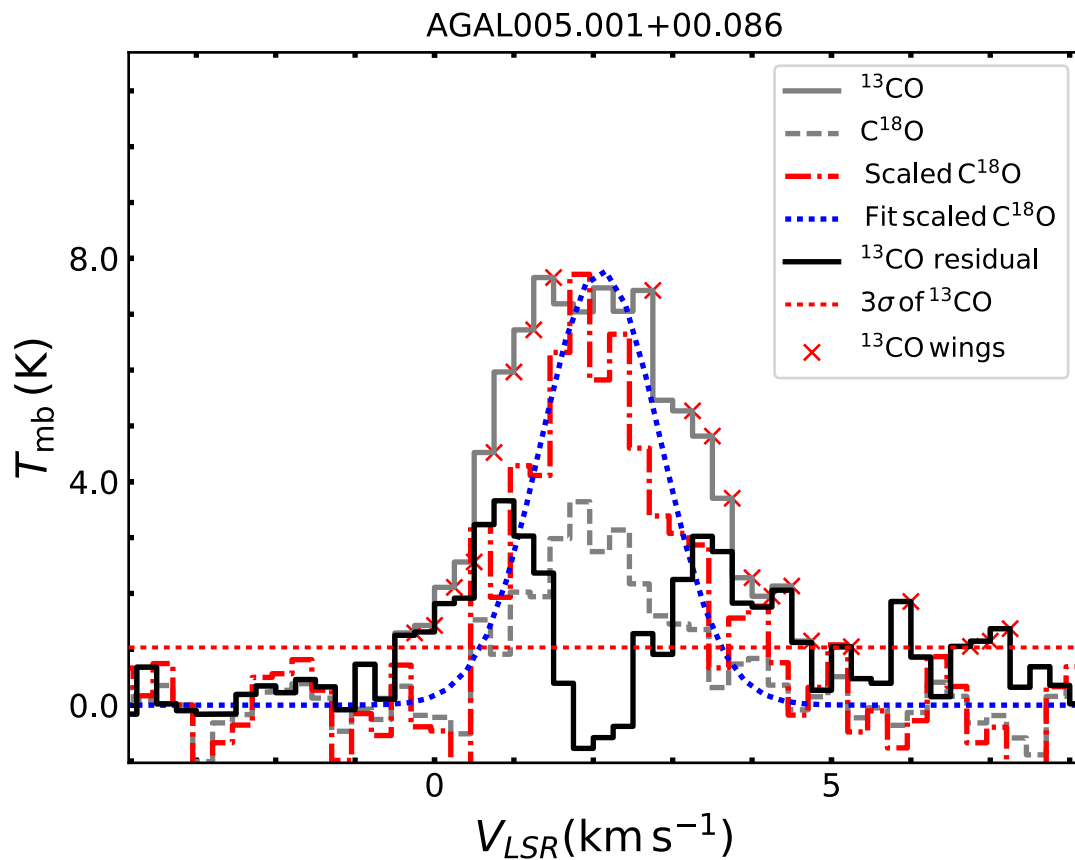
$$\beta_\tau = \frac{\Delta V}{\Delta V_{\text{int}}} = \frac{1}{\sqrt{\ln 2}} \left[ \ln \left( \frac{\tau_0}{\ln \left( \frac{2}{\exp(-\tau_0)+1} \right)} \right) \right]^{1/2}, \quad (4)$$

- $X_{\text{iso}} = \frac{N_{13\text{CO}}}{N_{\text{C18O}}} = 7.3$ ;
- $\frac{I_{\text{C18O}}}{I_{13\text{CO}}} = \tau_{\text{C18O}}$ ;
- $\tau_{13\text{CO}} = X_{\text{iso}} \tau_{\text{C18O}}$ ;
- 13CO optical thick & C18O optical thin;  
Ref: [Jimenez-Donaire+ 2017](#), Goldsmith+1984

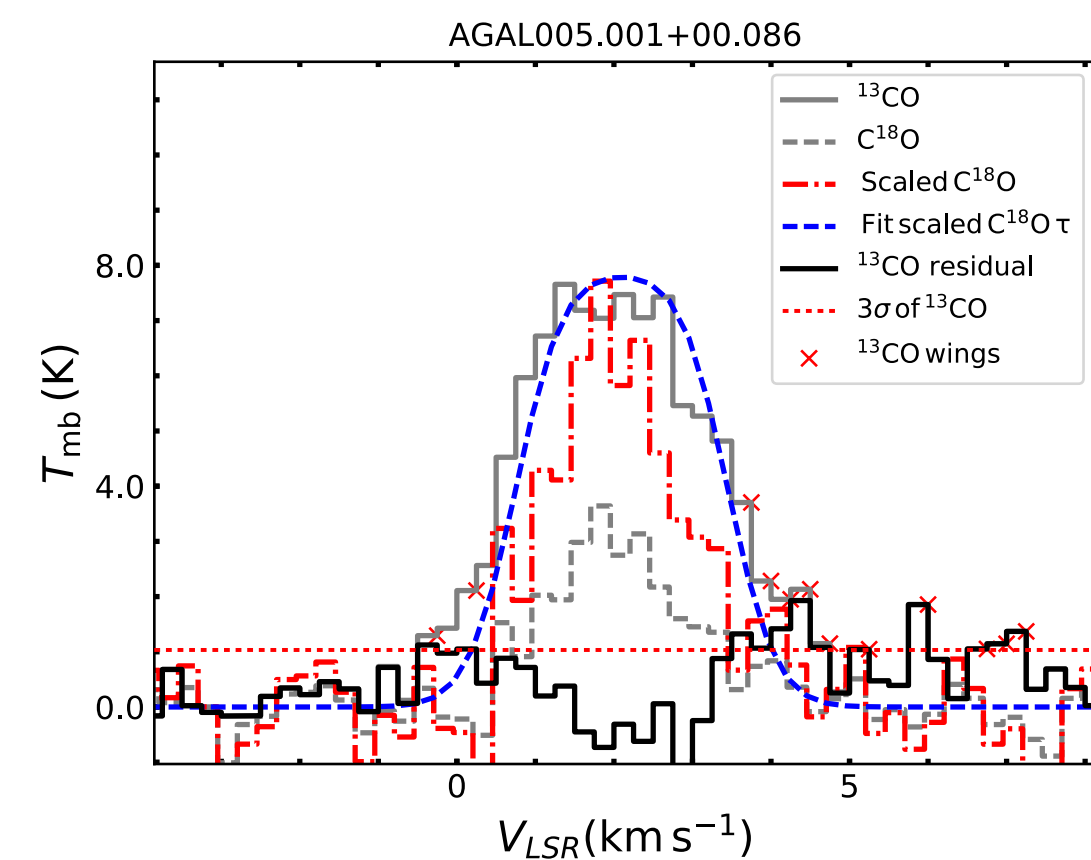


Max-Planck-Institut  
für Radioastronomie

- Outflows identification: after considering the opacity broadening



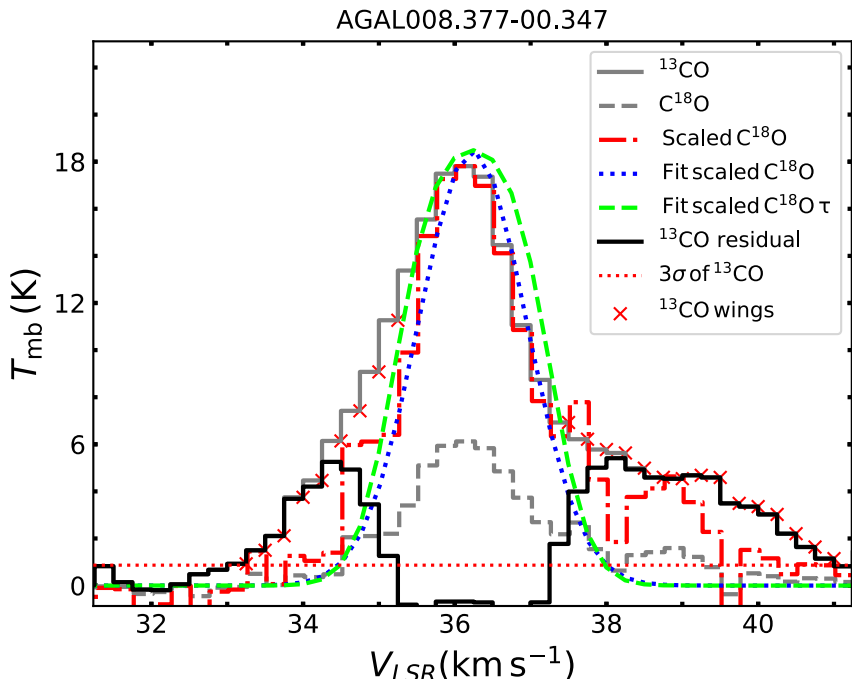
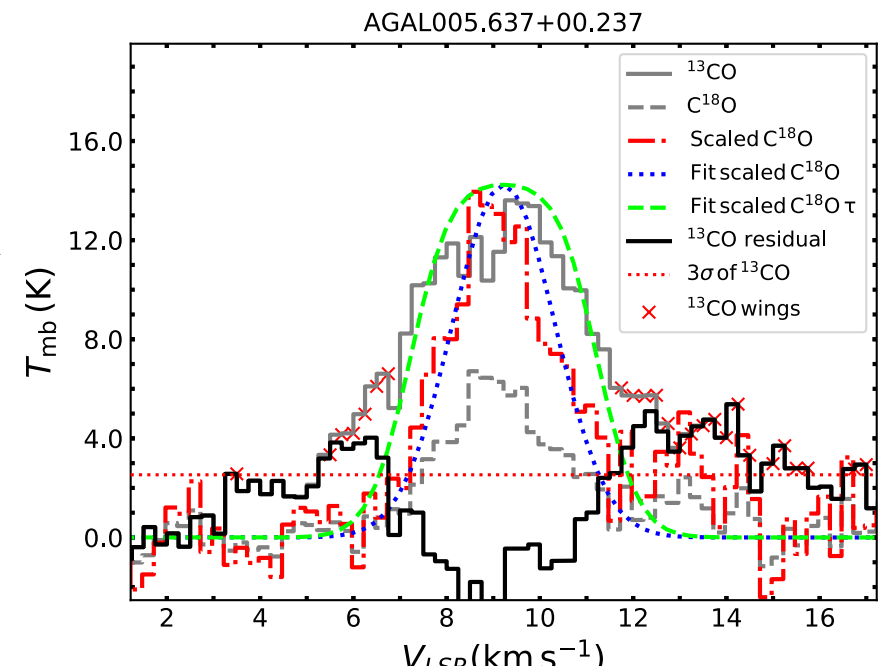
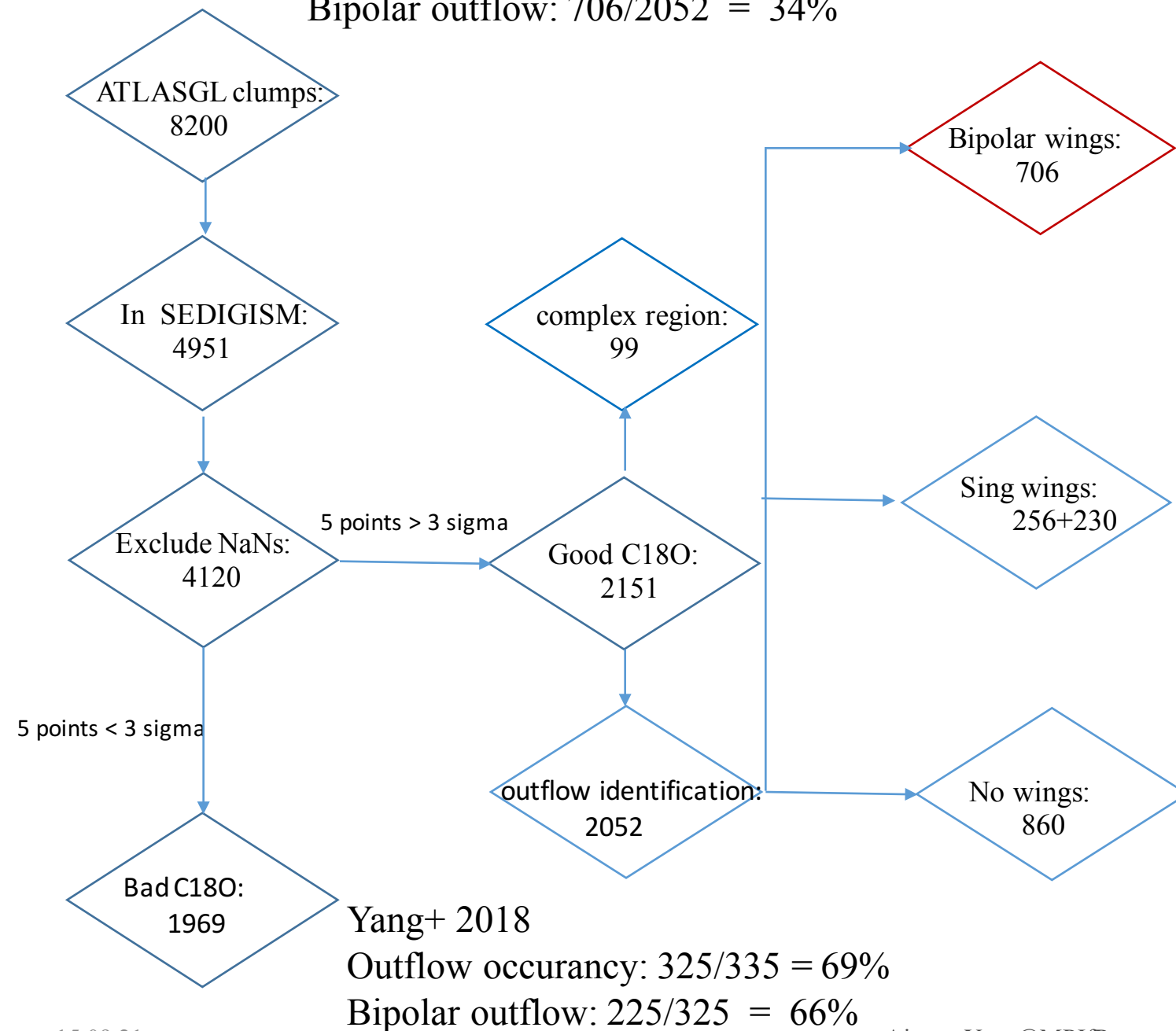
Not consider the opacity broadening



Consider the opacity broadening

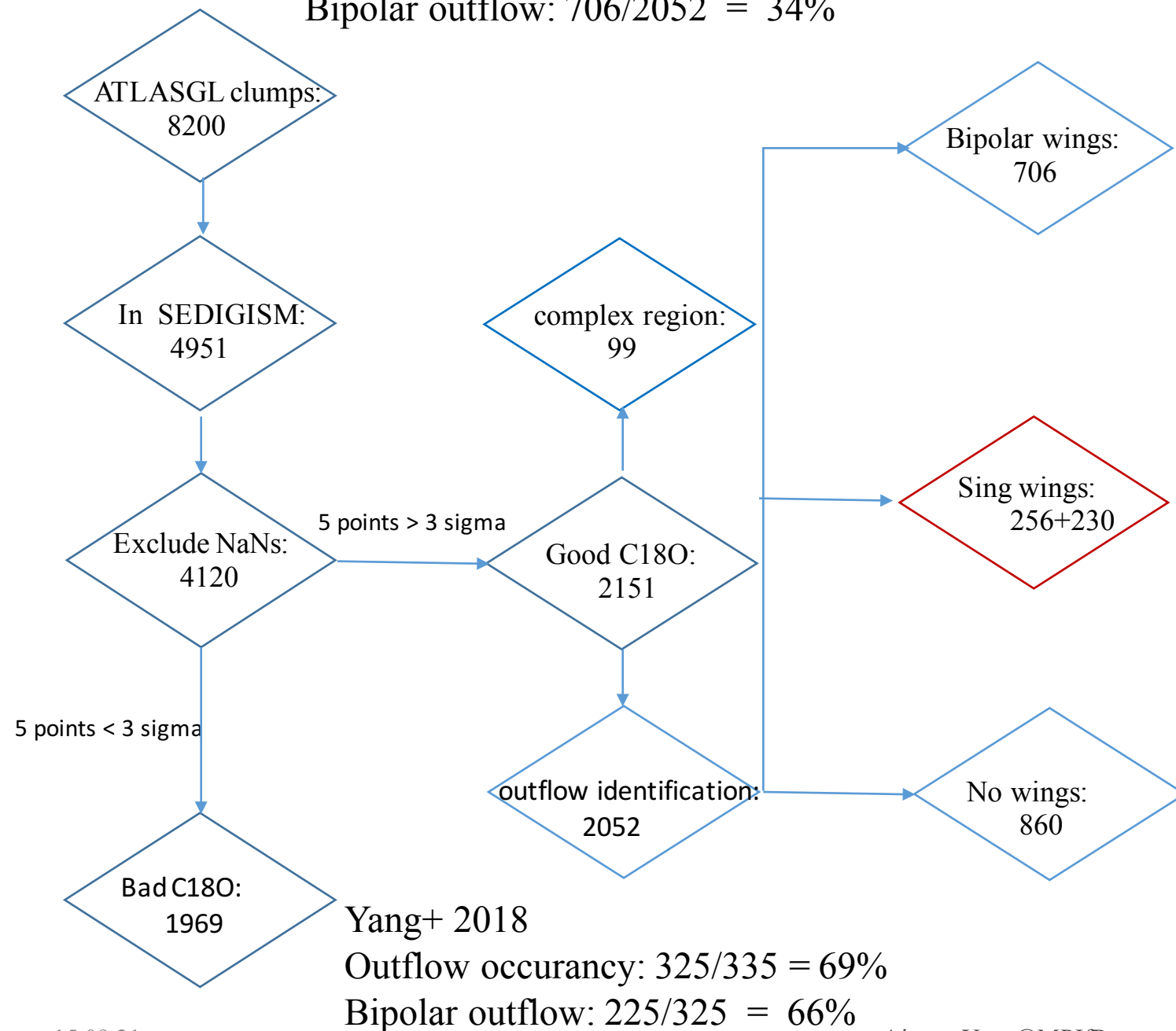
Outflow occupancy: 1192/2052 = 58%

Bipolar outflow: 706/2052 = 34%

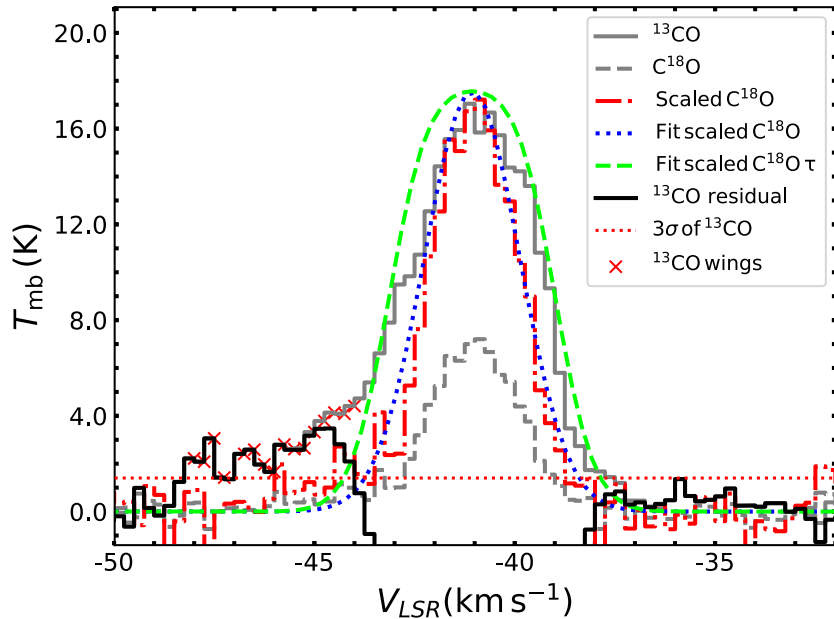


Outflow occurance: 1192/2052 = 58%

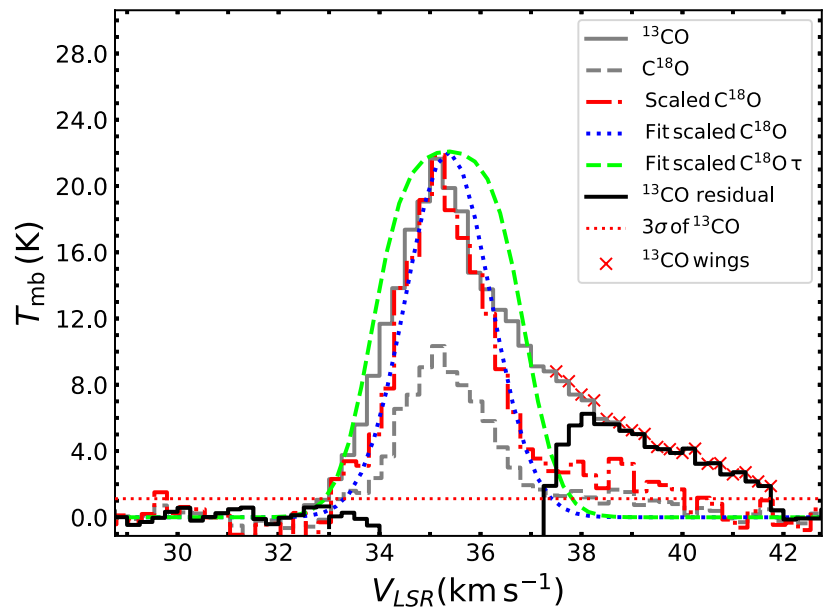
Bipolar outflow: 706/2052 = 34%

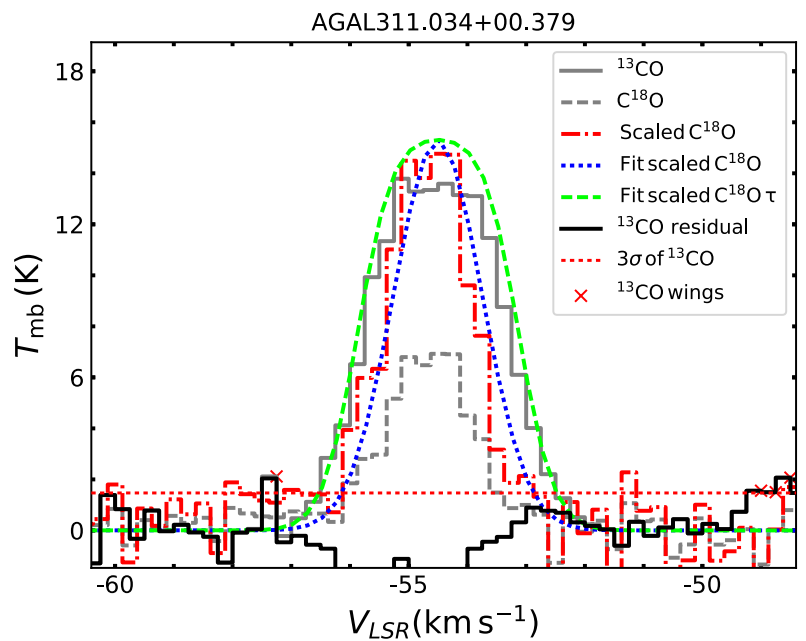
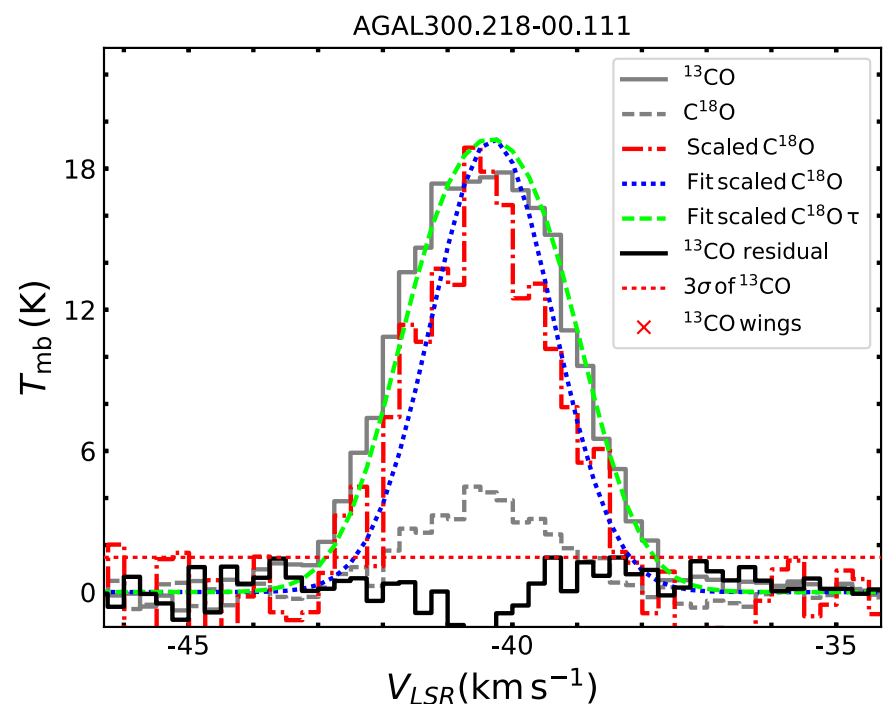
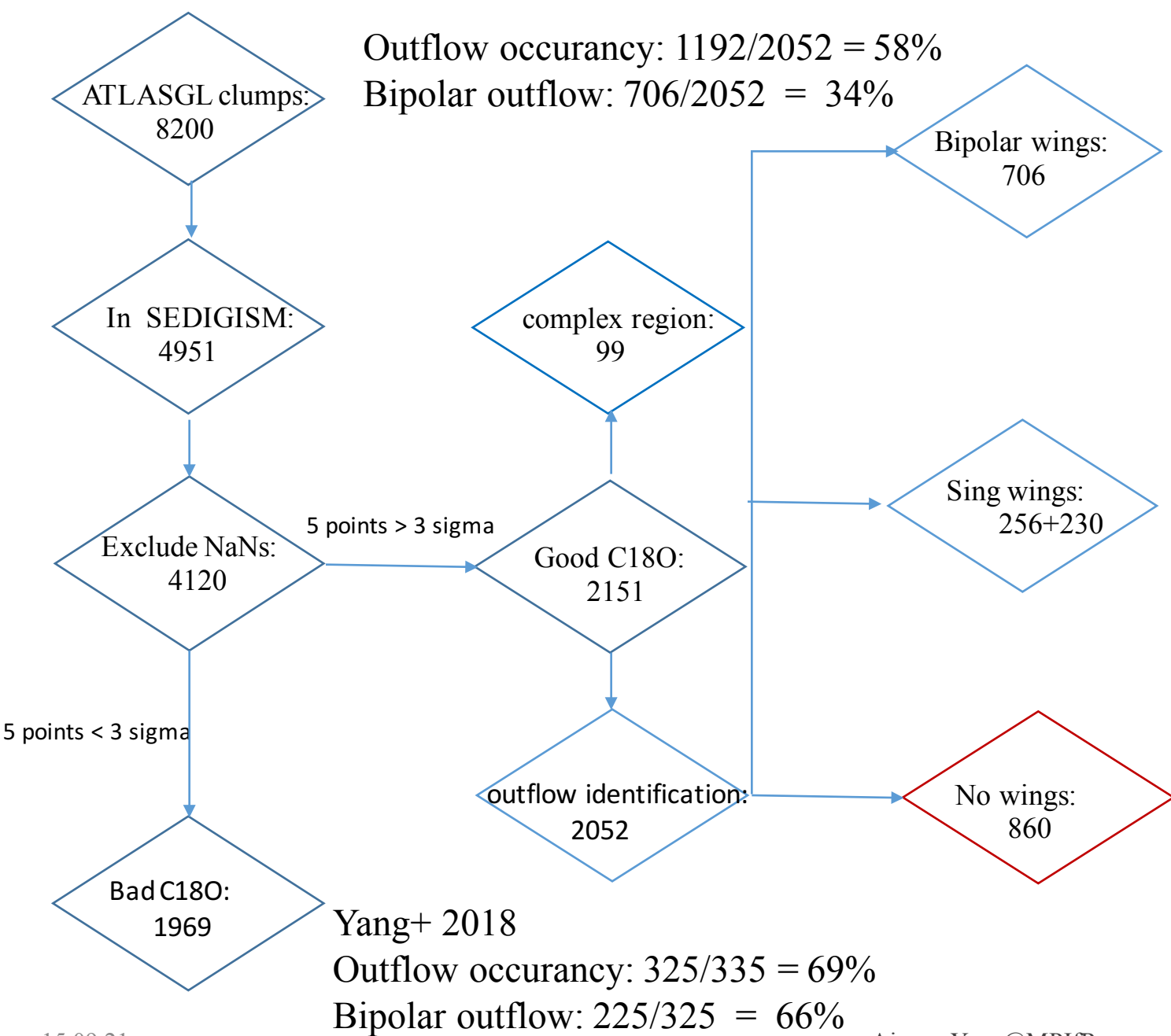


AGAL309.236-00.457



AGAL008.467-00.267



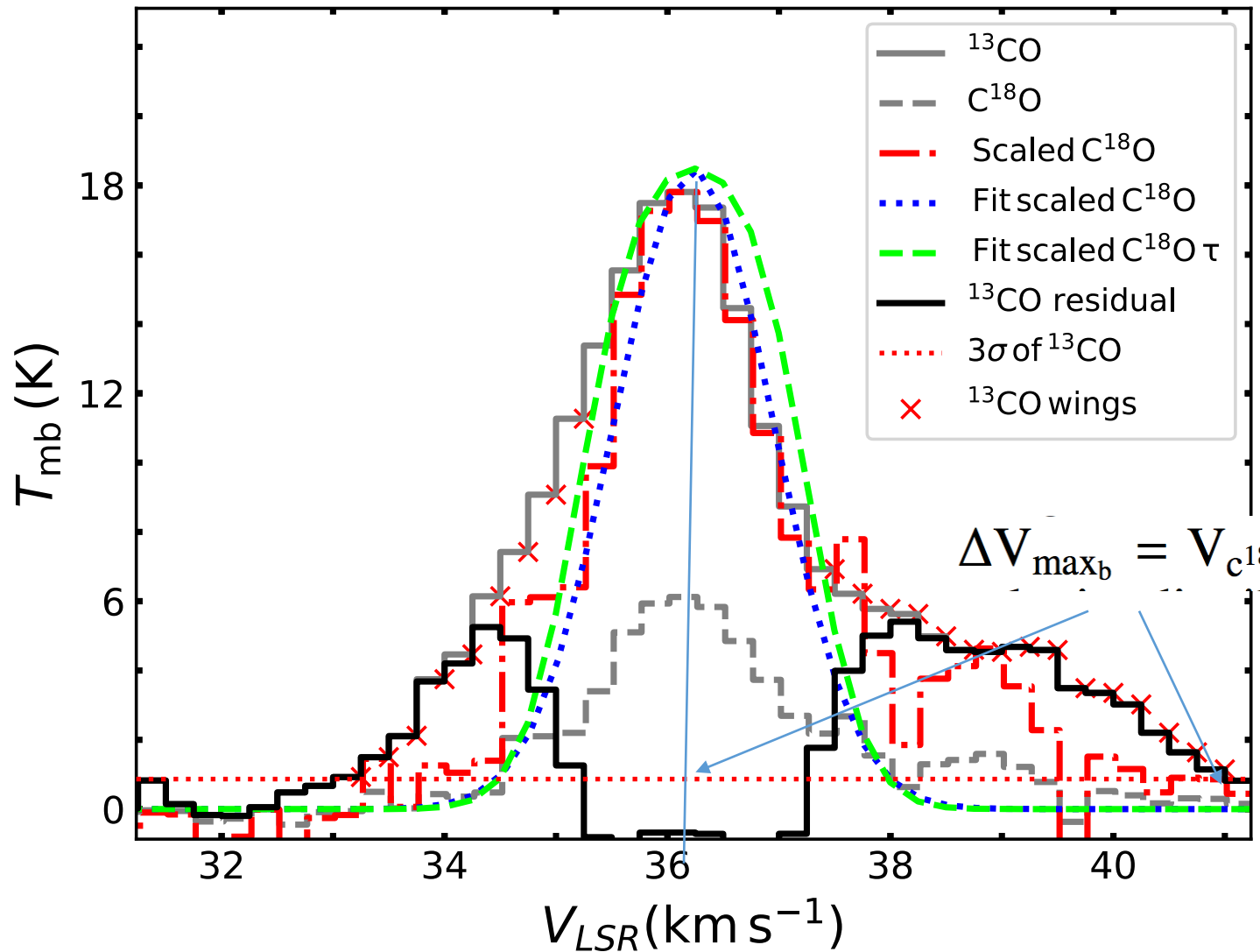


# Velocity ranges of the outflow wings



Max-Planck-Institut  
für Radioastronomie

AGAL008.377-00.347



Blue/Red velocity range  
 $\Delta V_{\text{max}}_{(\text{r/b})}$

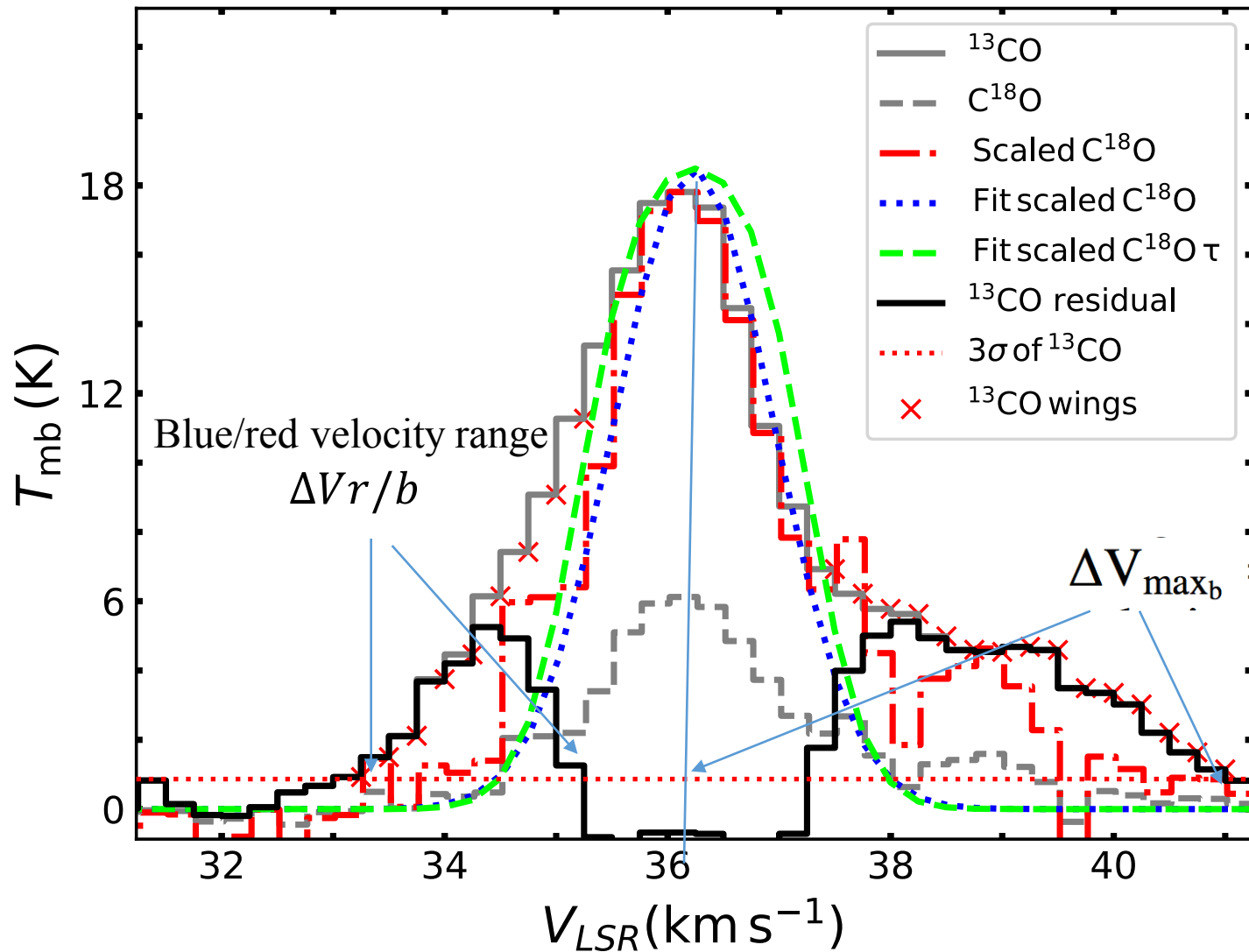
$$\Delta V_{\text{max}_b} = V_{\text{c}^{18}\text{O}} - V_{\text{min}_b} \text{ and } \Delta V_{\text{max}_r} = V_{\text{max}_r} - V_{\text{c}^{18}\text{O}}$$

# Velocity ranges of the outflow wings



Max-Planck-Institut  
für Radioastronomie

AGAL008.377-00.347

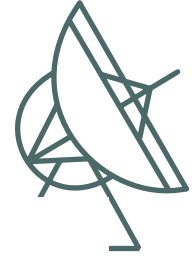


$$\Delta V_{b/r} = |V_{\max_{b/r}} - V_{\min_{b/r}}|$$

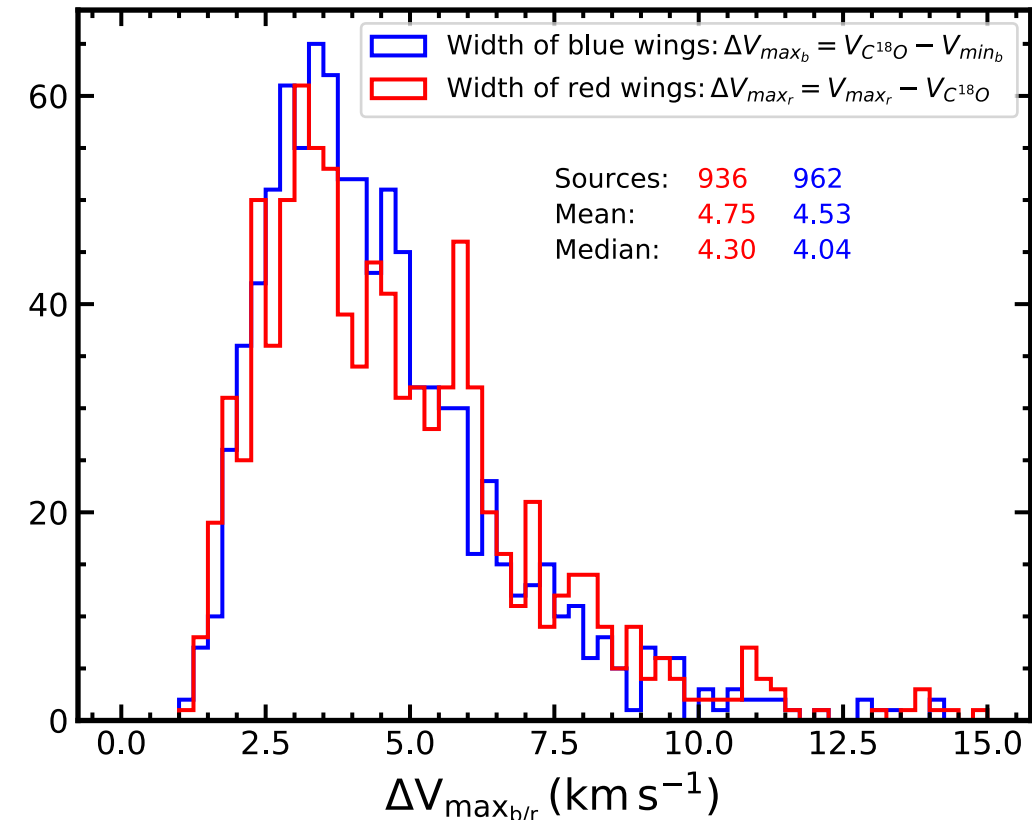
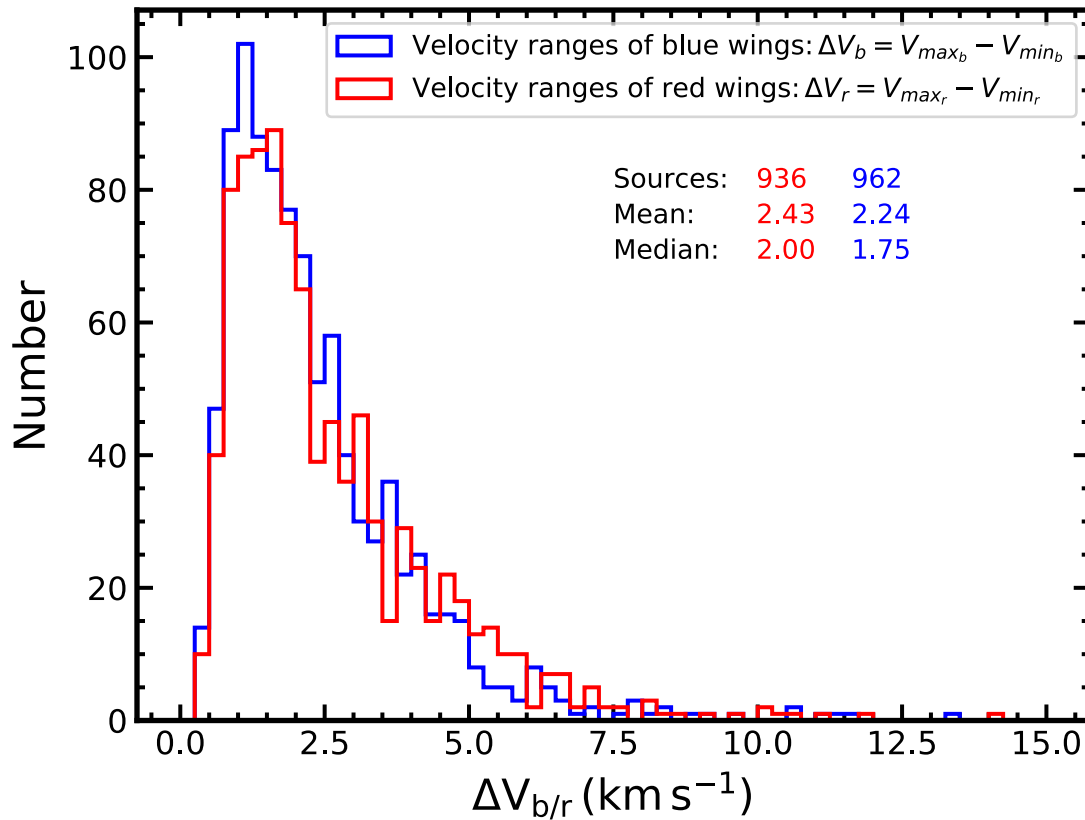
Blue/Red velocity range  
 $\Delta V_{\max_{(r/b)}}$

$$\Delta V_{\max_b} = V_{\text{c}^{18}\text{O}} - V_{\min_b} \text{ and } \Delta V_{\max_r} = V_{\max_r} - V_{\text{c}^{18}\text{O}}$$

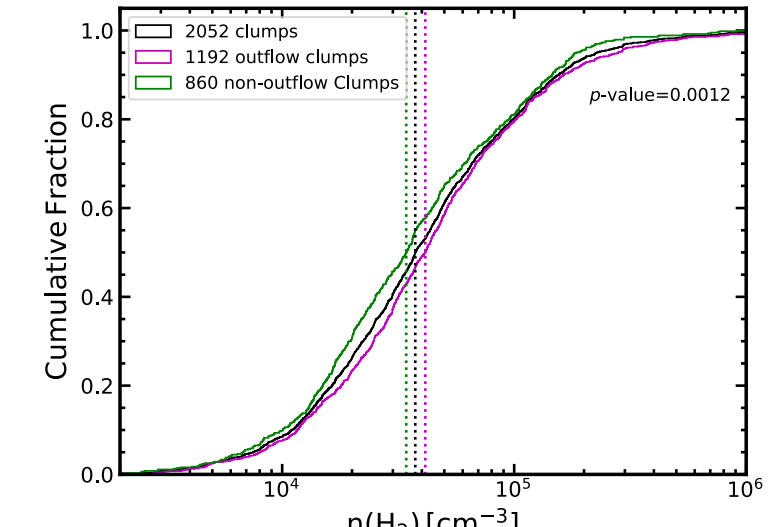
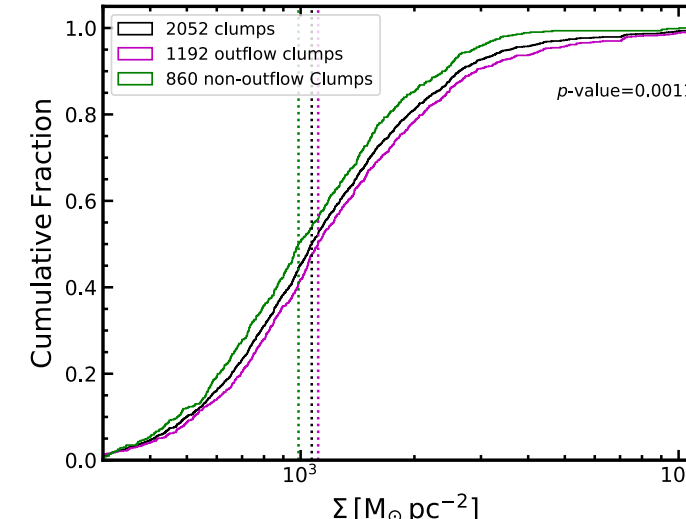
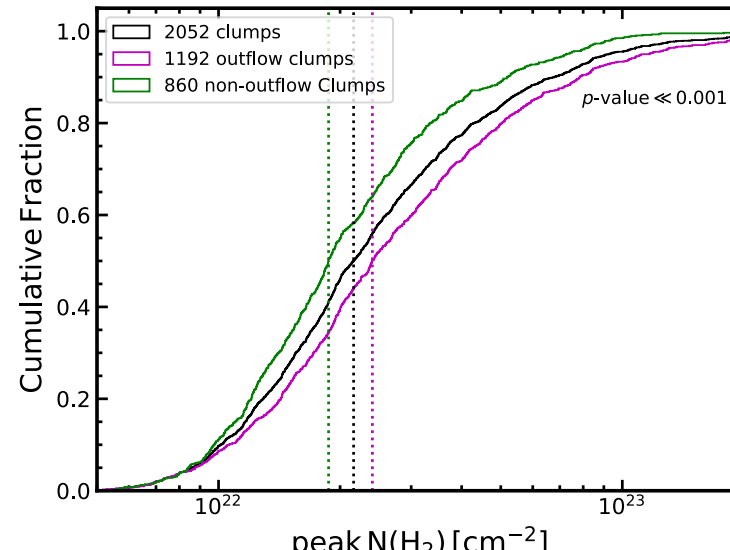
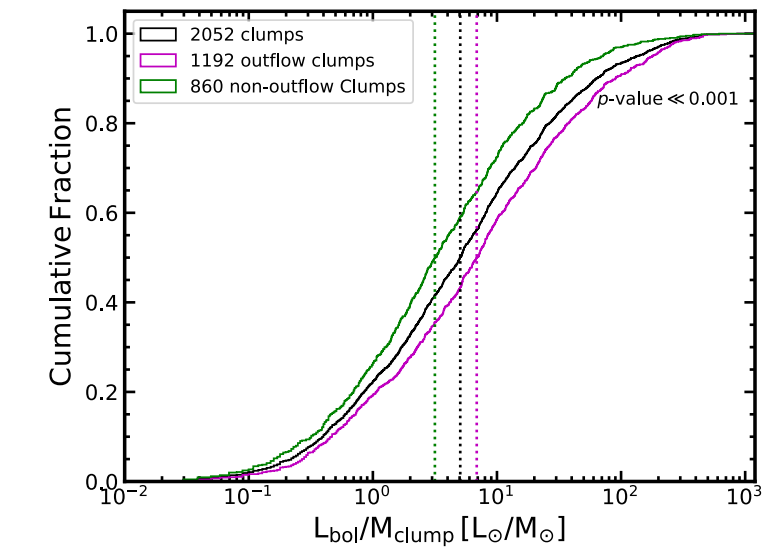
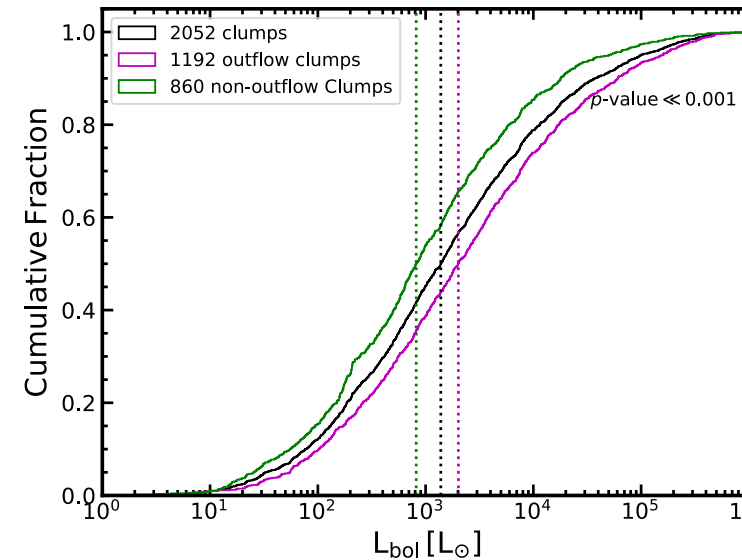
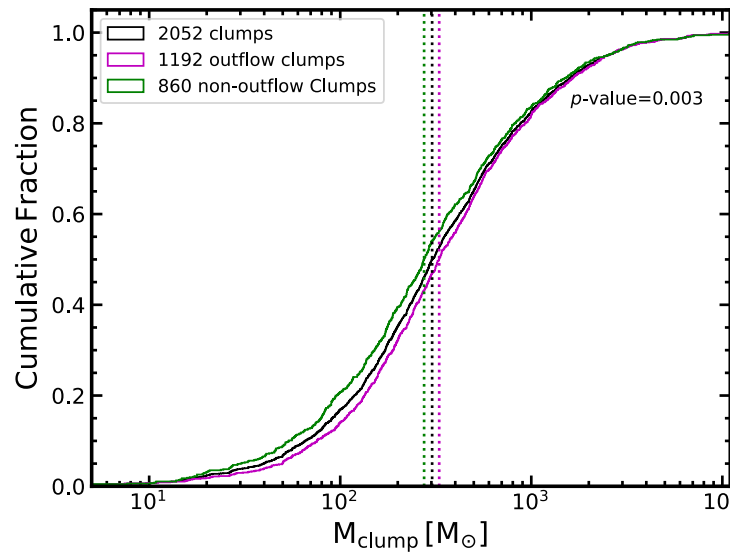
# Velocity ranges of outflow wings



–Institut  
astronomie



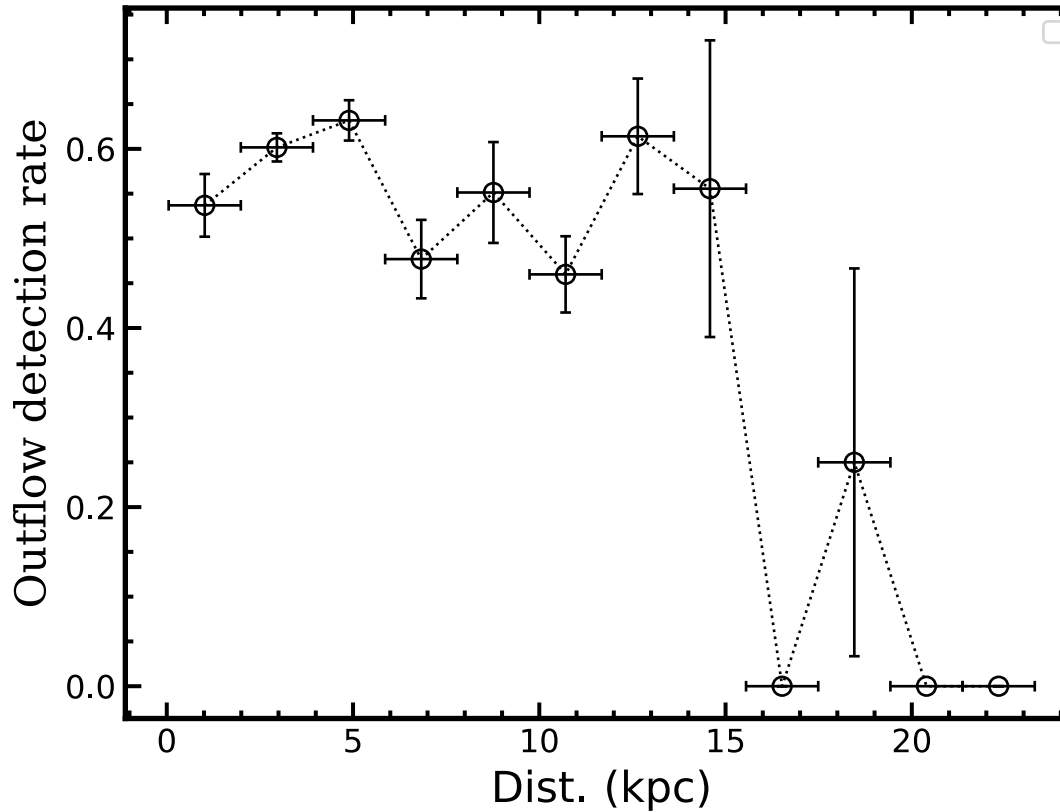
# Outflow clumps VS non-outflow clumps



# Outflow detection rate statistics

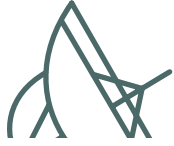


Max-Planck-Institut  
für Radioastronomie

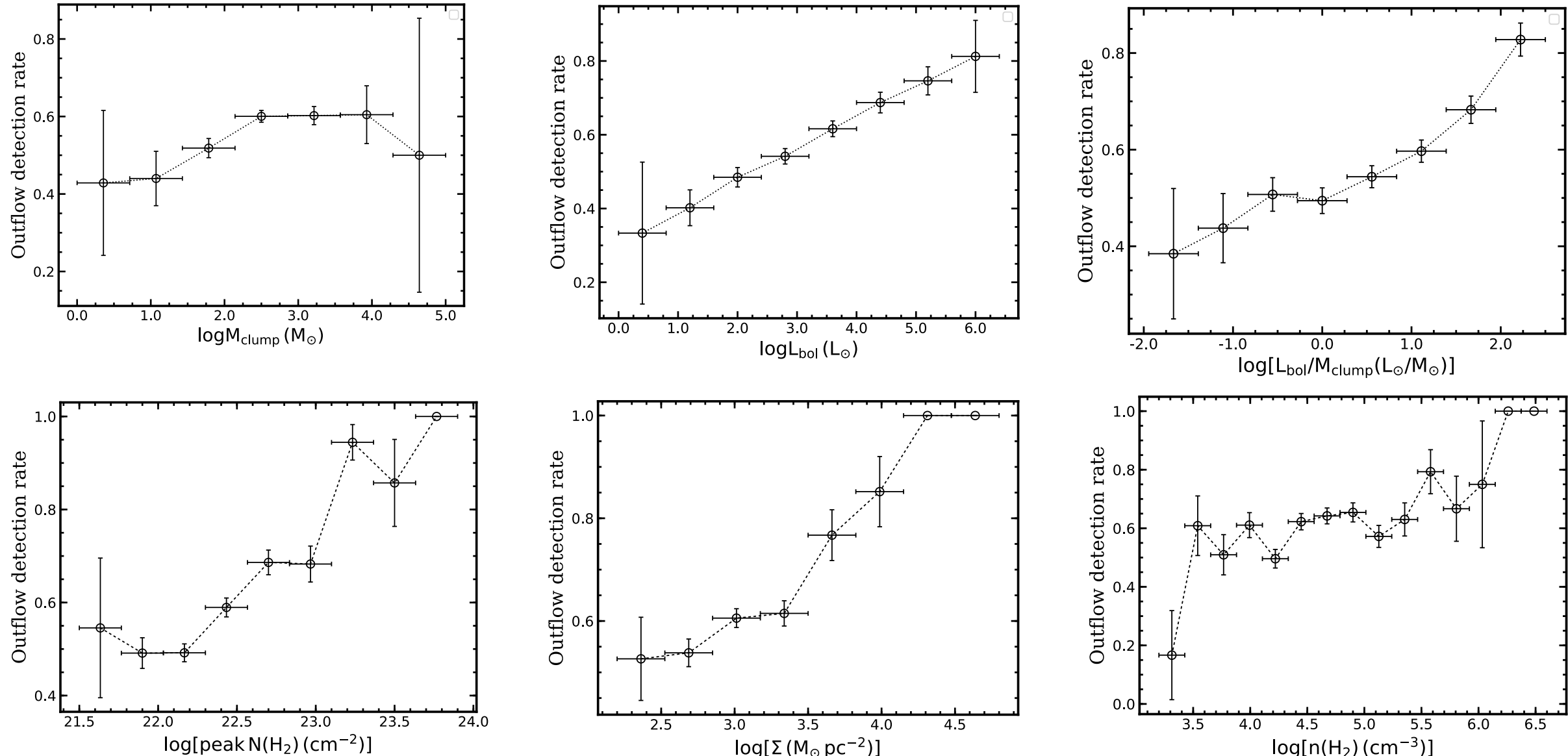


The detection rates are more or less similar for clumps with  $d < 1\text{,kpc}$  and sharply decrease when  $d > 14\text{ kpc}$ , however, only <1 % of the sources with  $d > 14\text{ kpc}$  in the sample.

The distances bias for the outflow identification wouldn't be significant and the systematical analysis of the detection rate is valid.



# Outflow detection rate statistics

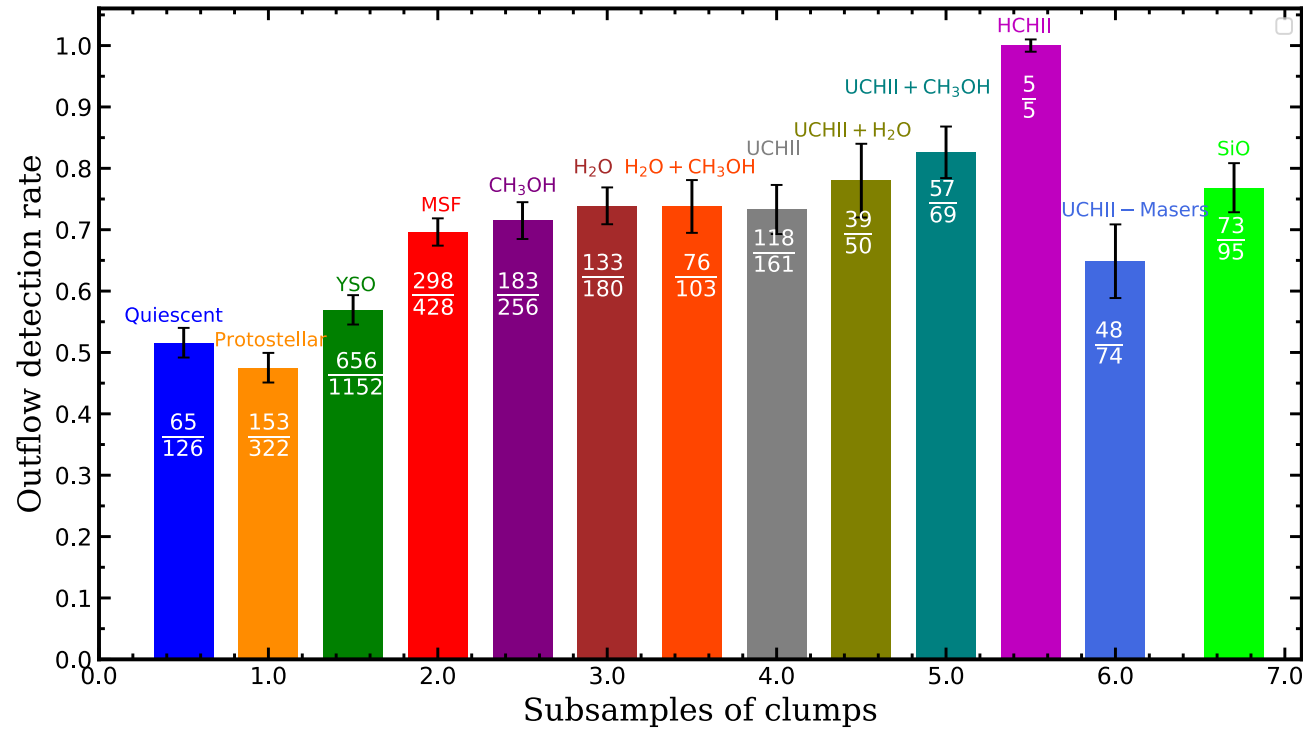


# Outflow detection rate statistics

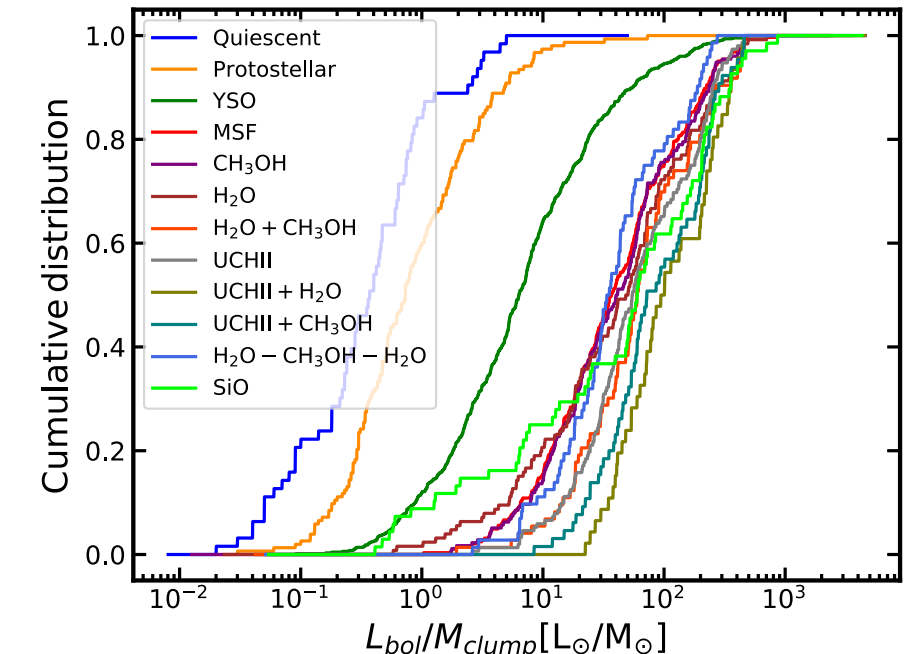
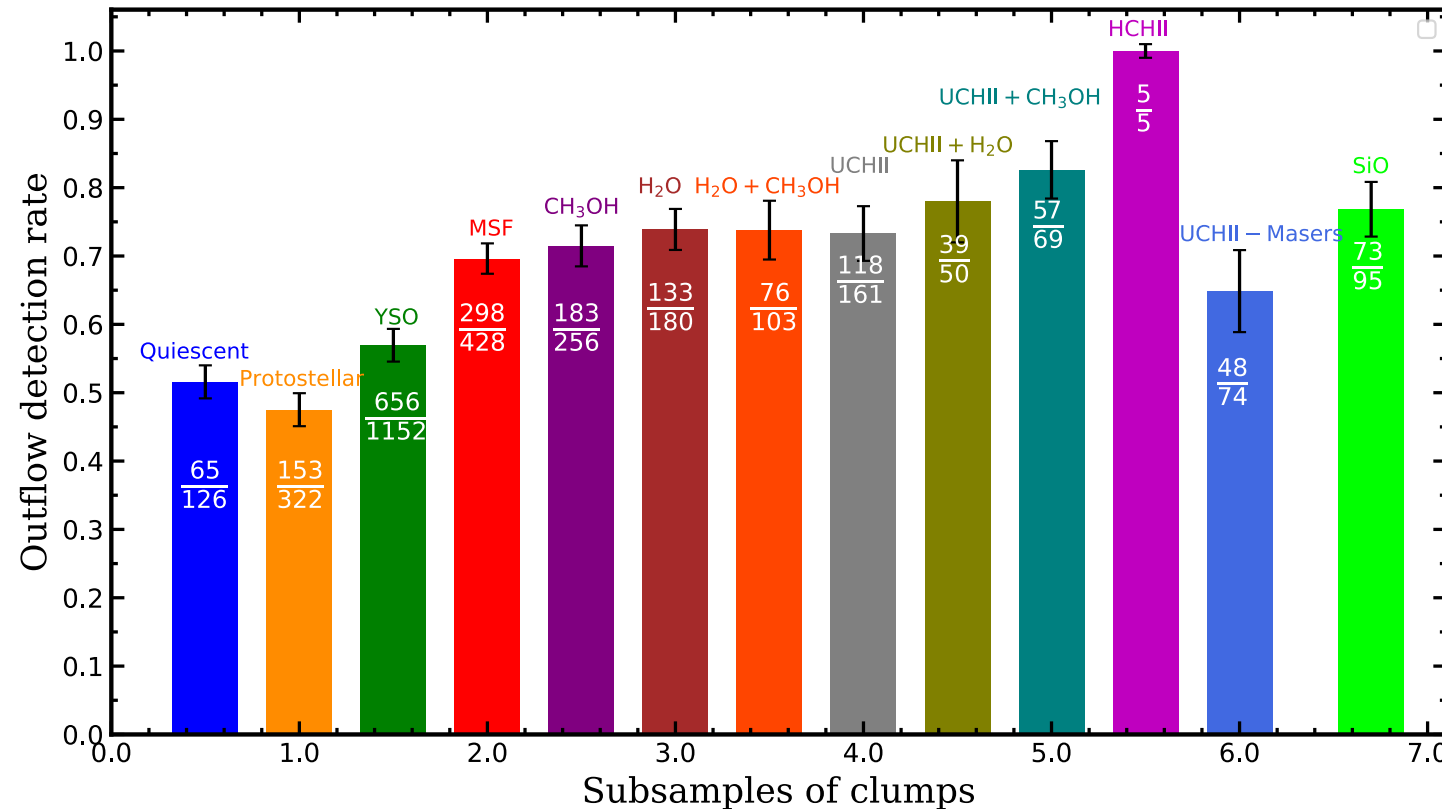


**Table 4.** Results of outflow detection rate for clumps in different evolutionary stages.

Clumps	Number	With outflow
Total	2052	1192 (58%)
Quiescent	126	65 (51%)
Protostellar	322	153 (47%)
YSO	1152	656 (57%)
MSF	428	298 (70%)
SiO	95	73 (77%)
CH <sub>3</sub> OH Masers	256	183 (71%)
H <sub>2</sub> O Masers	180	133 (74%)
CH <sub>3</sub> OH + H <sub>2</sub> O	103	76 (74%)
UCH II regions	161	118 (73%)
UCH II +H <sub>2</sub> O	50	39 (78%)
UCH II +CH <sub>3</sub> OH	69	57 (86%)
HC H II regions	5	5 (100%)
UCH II -Masers	74	48 (65%)



# Outflow detection rate statistics

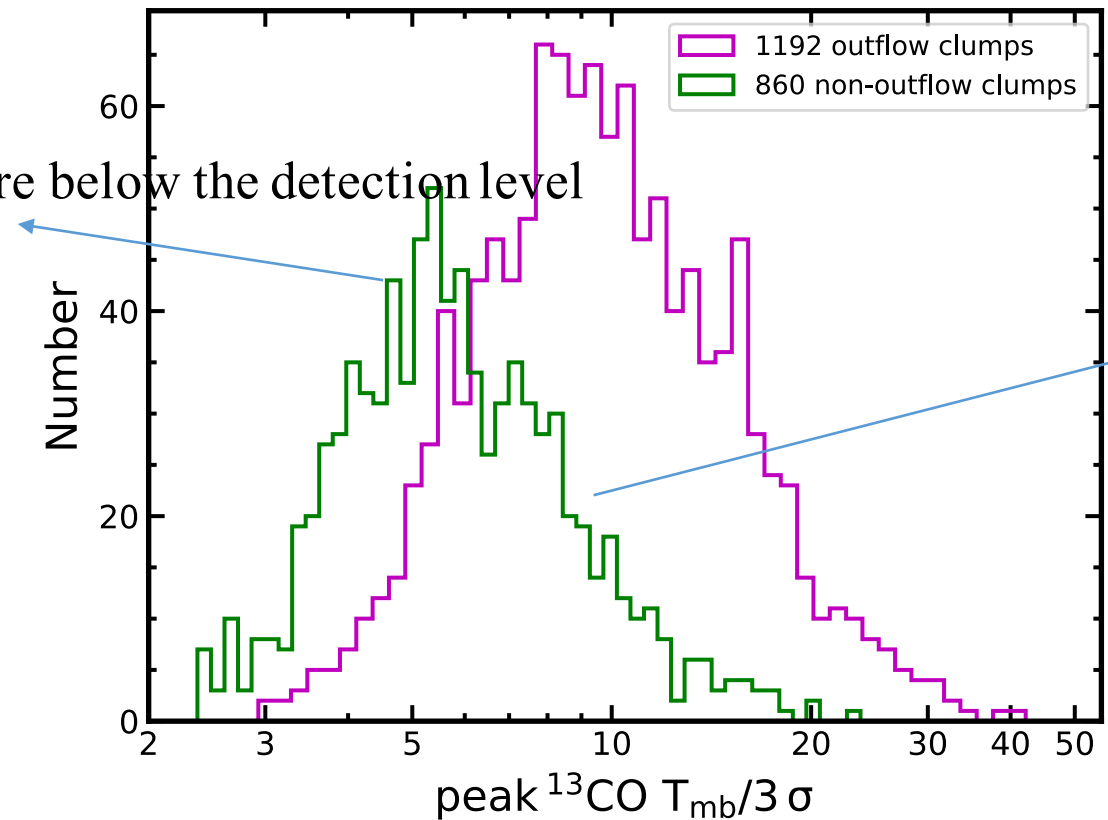


# detectability



Max-Planck-Institut  
für Radioastronomie

non-outflow sources,  
or have weak wings that are below the detection level

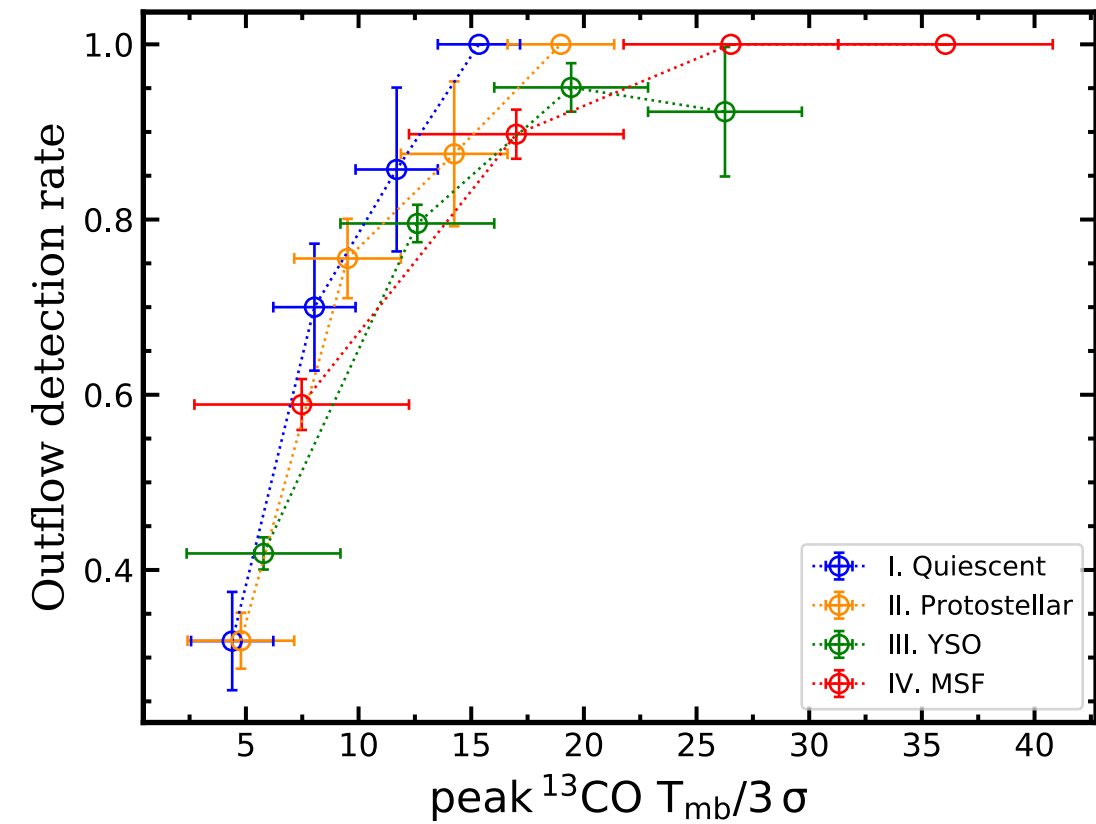
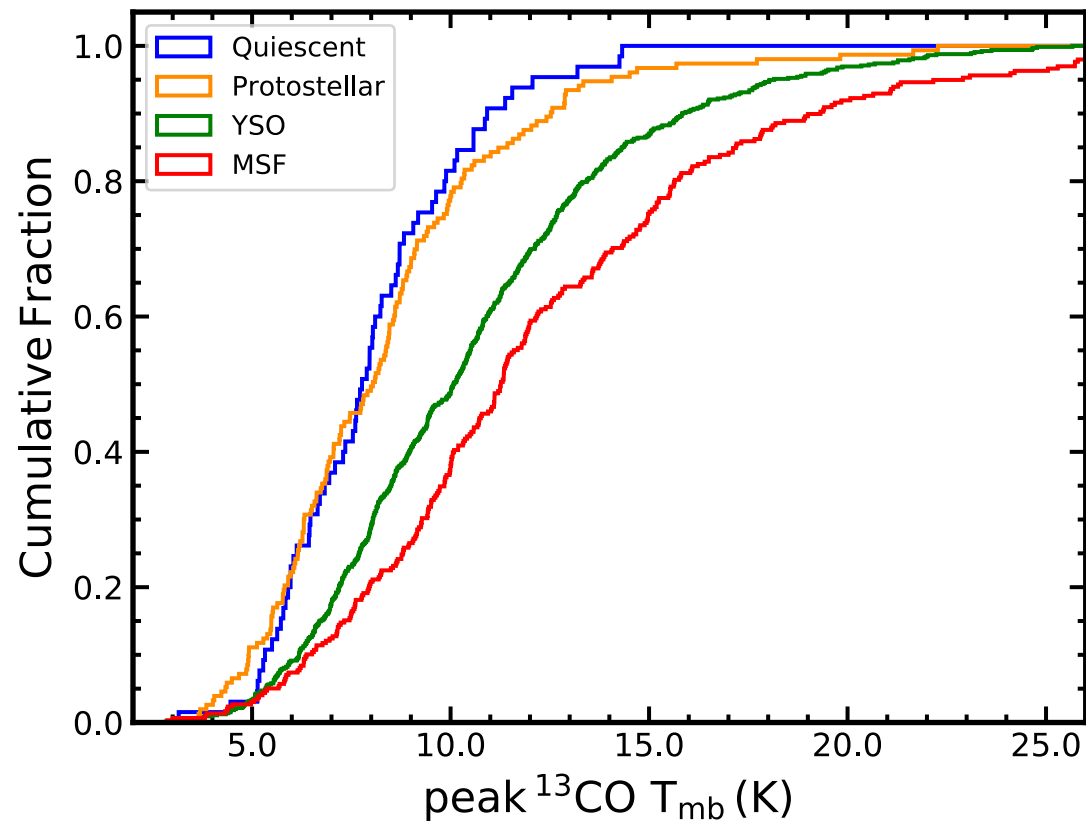
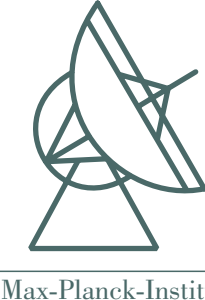


non-outflow sources,  
or have wings that cannot be detected

The non-outflow sources shows a lower peak value than the outflow sources, indicating that part of the sources without wings (and hence classified as non-outflow sources) could just have wings that fall below the noise level.

# detectability

Are the increase in detection rate significant?



# Furture aspects



Max-Planck-Institut  
für Radioastronomie

## 1, Follow-up SiO line survey toward the outflow clumps

The outflow identification process can be affected by:

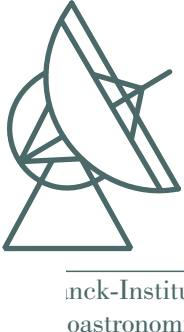
- 1, confusion (the observed sources lie along the Galactic plane where most of the molecular material resides)
- 2, spectral noise (in the case of weak sources);
- 3, outflow geometry;
- 4, the beam filling factor of CO line emission;
- 5, the opacity variations in the CO line wings;

→it is possible to miss outflows or mis-identification

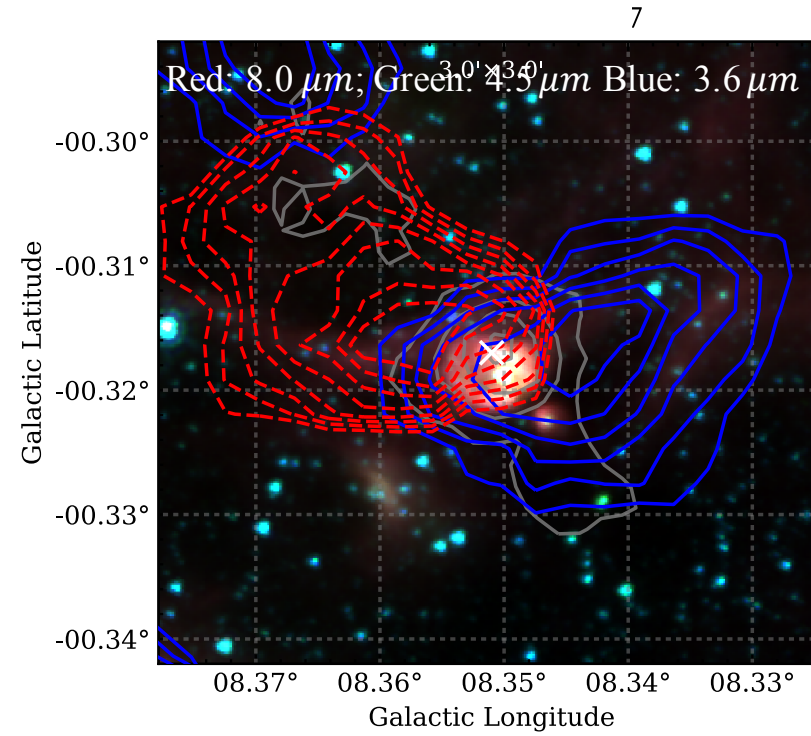
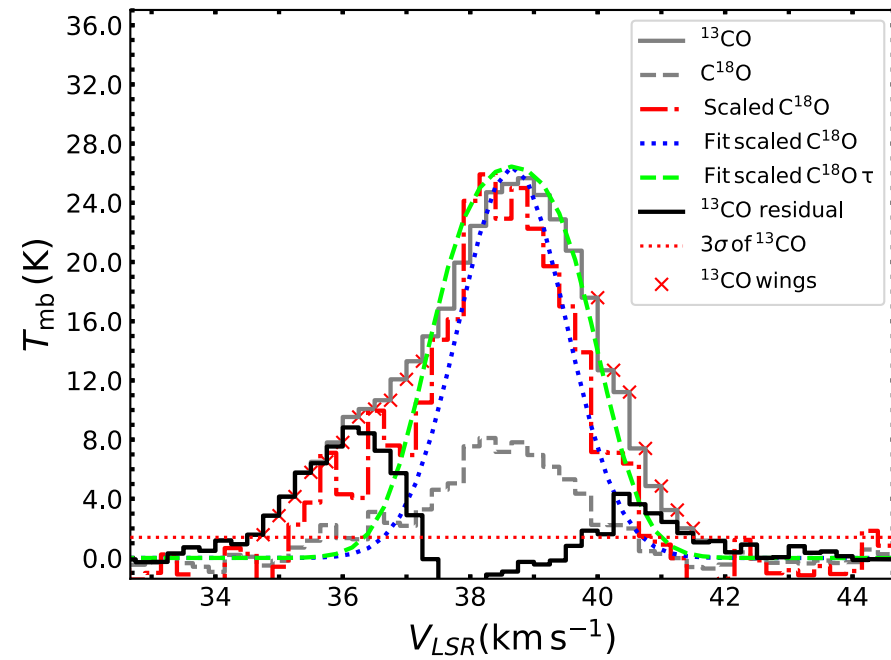
Unlike CO, SiO emission suffer much less from confusion with ambient material, and would be a better traces of outflows.

The observation of SiO toward the sample allows us to obtain a more rigorous sample of outflow clumps.

# Future prospects



## 2, Outflow mapping at higher resolution:

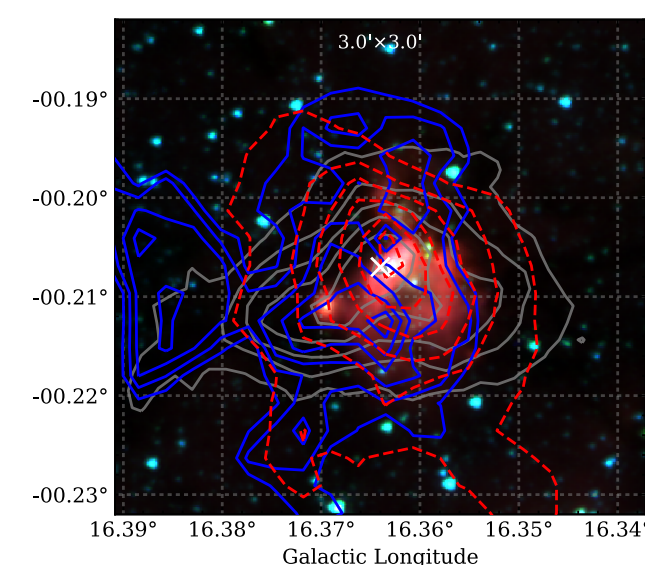
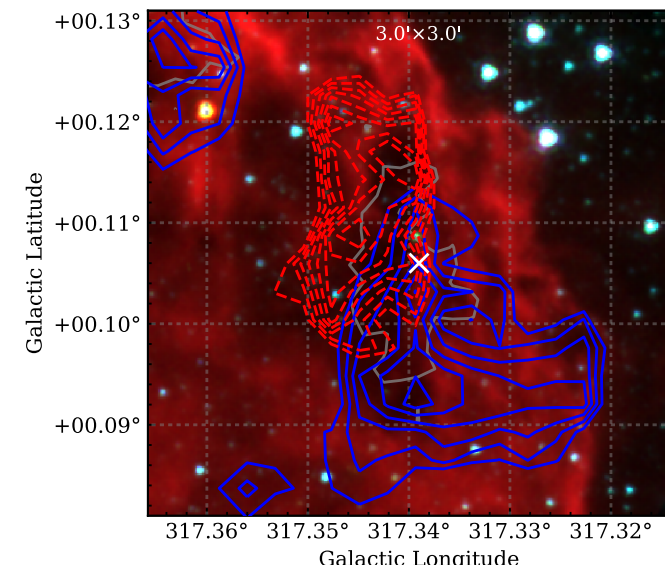
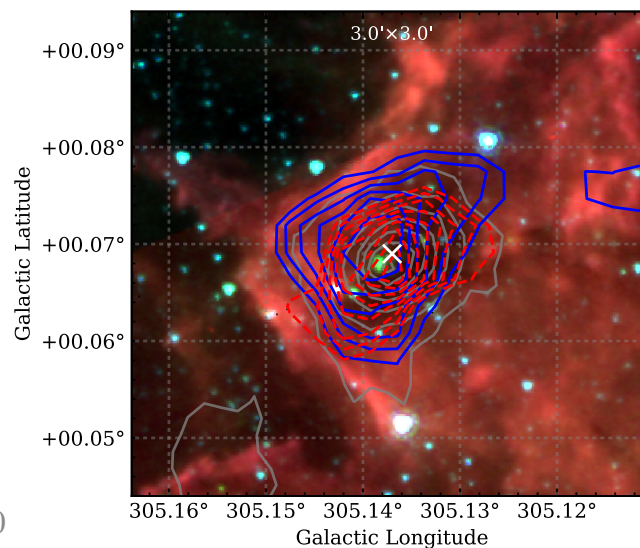
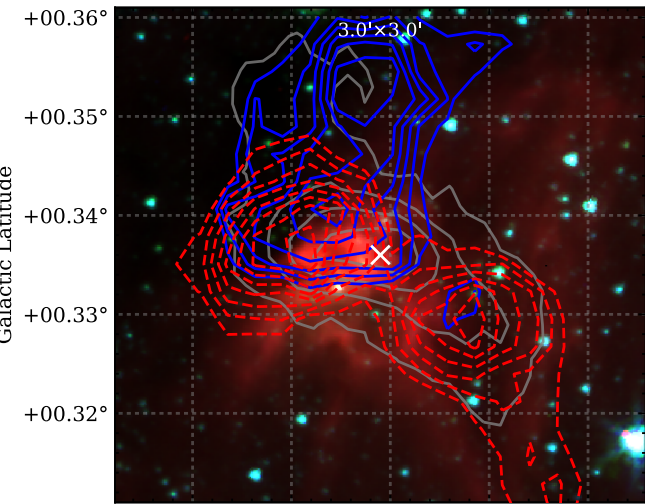
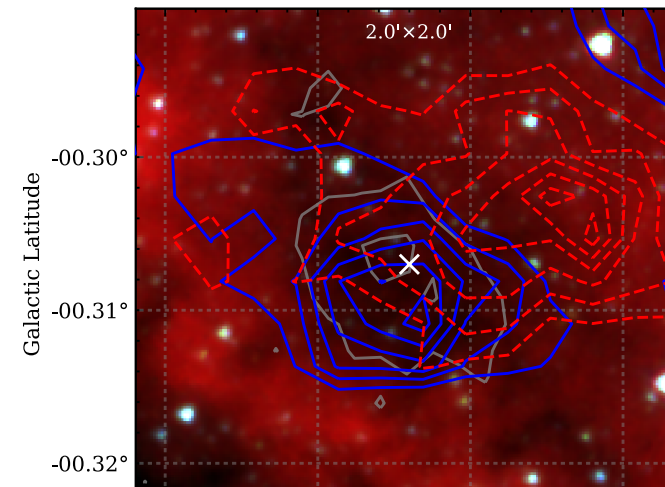
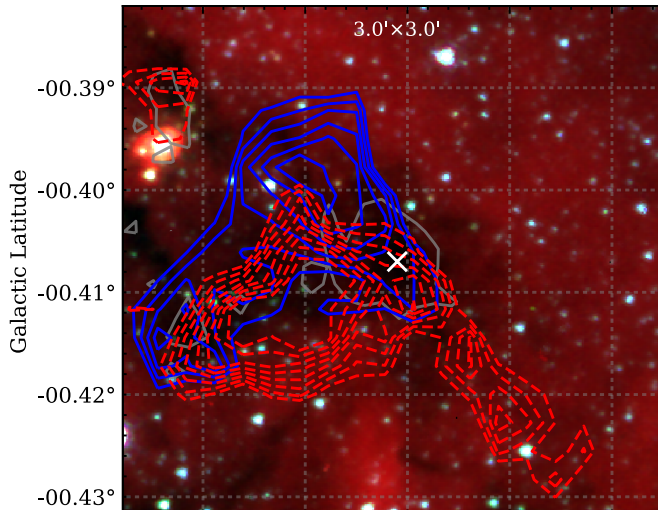


7



# Future prospects

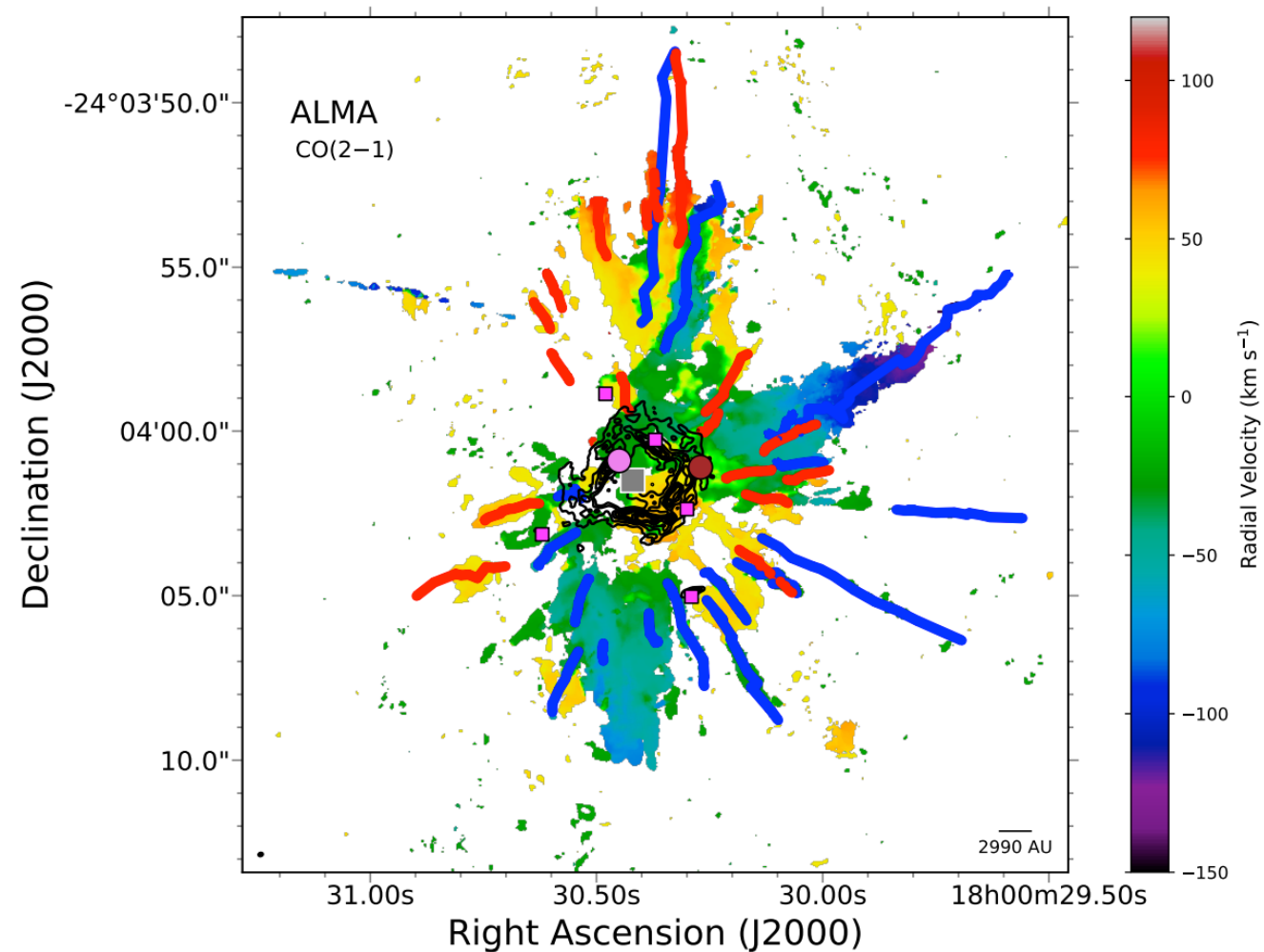
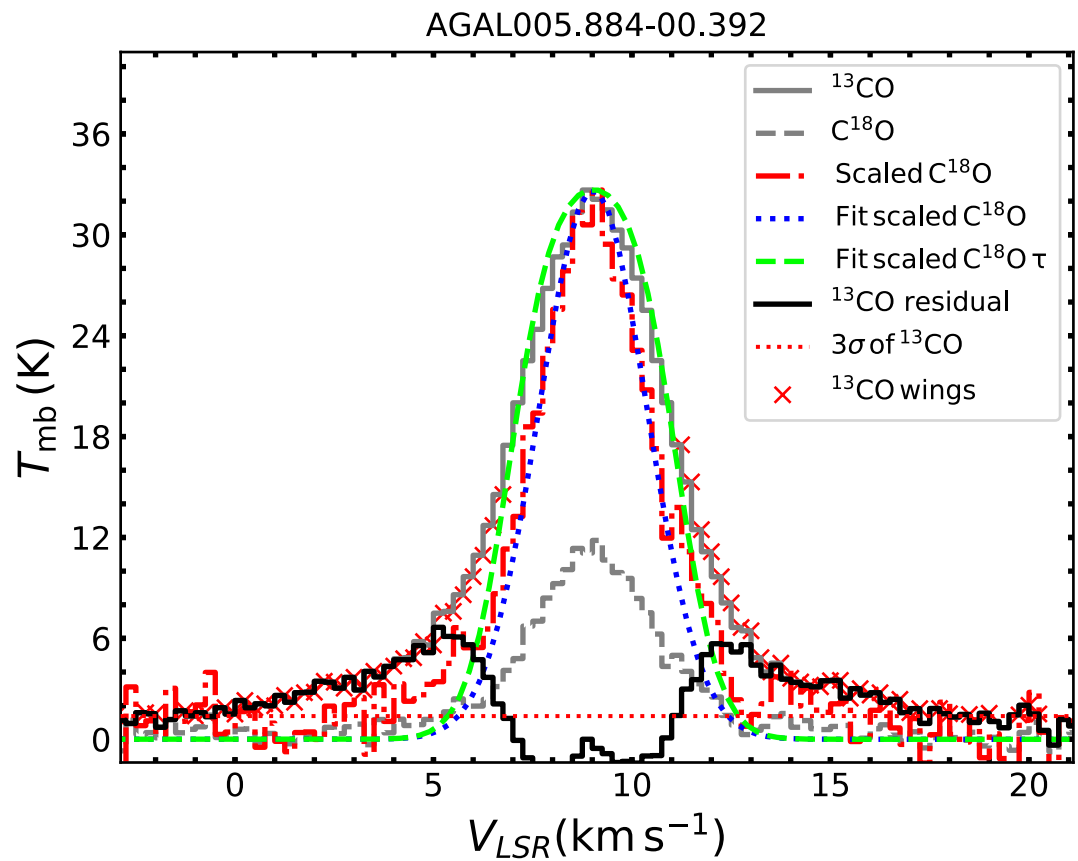
Outflow mapping at higher resolution:



# Future prospects



Extremely high-velocity outflow source? Explosive Outflow?



Zapata+ 2019,2020

# Future prospects

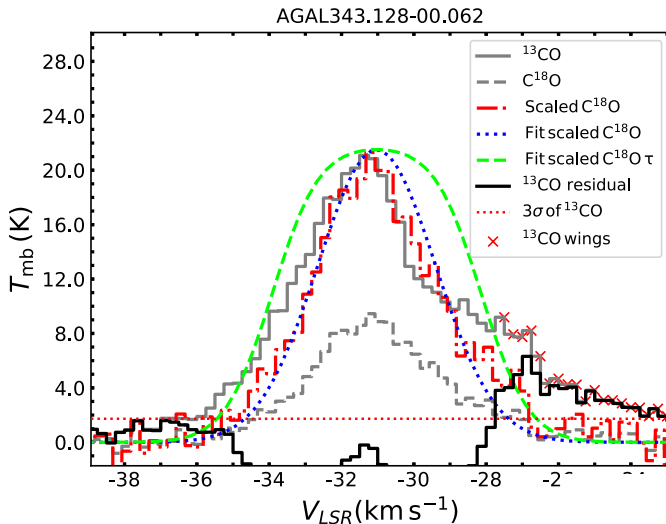
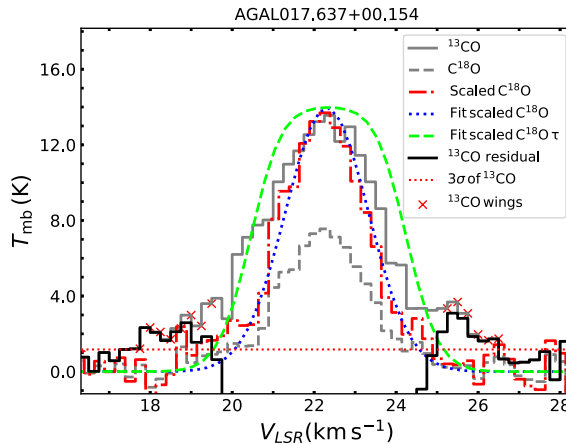
## Keplerian disc candidates around O-type high-mass stars?

**Table 3.** Properties of Keplerian disk candidates around HMYSOs as observed with ALMA to date.

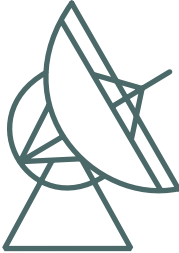
Object	Distance	Luminosity	Star Mass	Disk Mass	Disk Radius	References
	[ kpc ]	[ $L_\odot$ ]	[ $M_\odot$ ]	[ $M_\odot$ ]	[ AU ]	
B-type YSOs						
Orion Source I	0.4	$\sim 10^4$	$15 \pm 2$	$< 0.2$	75-100	[1,2]
IRAS 20126+4104	1.6	$\sim 10^4$	12	1.5	860	[3,4]
IRAS 18162–2048 <sup>a</sup>	1.7	$\sim 10^4$	18	4	300	[5]
G339.88-1.26	2.1	$4 \times 10^4$	$11 \pm 5$	—	430–630	[6]
G35.20-0.74N	2.2	$\sim 10^4$	$18 \pm 3$	3	2500	[7]
G35.03+0.35 A	3.2	$6 \times 10^3$	$9 \pm 4$	0.75	2200	[8,9]
G16.59–0.05	3.6	$3 \times 10^4$	$10 \pm 2$	$1.8 \pm 0.3$	500	[10]
O-type YSOs						
S255IR NIRS3	1.8	$1.6 \times 10^5$ <sup>b</sup>	20	0.3	500	[11]
G351.77-0.54	2.2 <sup>c</sup>	$1.7 \times 10^4$	14-25 <sup>d</sup>	0.1-0.49 <sup>e</sup>	250-500 <sup>b</sup>	[12]
G17.64+0.16	2.2	$\sim 10^5$	$45 \pm 10$	$< 2.6$	120	[13,14]
IRAS16547-4247	2.9	$\sim 10^5$	20	4	870	[15,16]
G11.92-0.61 MM1	3.4	$\sim 10^4$ <sup>f</sup>	$34 \pm 5$	2.2-5.8	480	[17]
AFGL 4176	4.2	$\sim 10^5$	20	2-8	1000	[18,19]
G023.01-00.41	4.6	$4 \times 10^4$	20	1.6	2500	[20]

NOTE— When mass error bars are not given, the measurements should be taken as loose estimates, e.g., based on consistency checks between a stellar type and the upper-limit luminosity. Radius estimates are wavelength-dependent.

Goddi+2019



# Summary



Max-Planck-Institut  
für Radioastronomie

- Outflow is a common activity in the massive star formation process
  - 1192 clumps out of the 2052 show outflows~ 58%, 34% for bipolar wings; 24% for unipolar wings
  - higher values for HCHII(100%), UCHII(93%), Masers(84%).
- Outflow switches on the youngest stages of clump i.e.  $70 \mu\text{m}$  dark;
- Obtain a sample of sources in the  $70 \mu\text{m}$  dark and 24 dark phases;
- Outflow detection rate increases as clumps evolve, the increasing of L;
  - From Prestellar(51%), Protostellar (47%), YSO-forming(58%), MSF(70%)
- However, the increase in detection rate are more likely to be due to an increase in detectability rather than a lower fraction of outflow frequency.
- This is the largest outflow sample so far, providing interesting targets: (1)  $70 \mu\text{m}$  dark outflow clumps, and (2) extremely high-velocity outflow clumps



Max-Planck-Institut  
für Radioastronomie

Thank you very much for your attention~